Journal of Chromatography A, 1217 (2010) 792–812

Contents lists available at ScienceDirect

Journal of Chromatography A

journal homepage: www.elsevier.com/locate/chroma

Review

Characterization of adsorption processes in analytical liquid–solid chromatography

Torgny Fornstedt*

Department of Physical and Analytical Chemistry, Uppsala University, BMC Box 599, SE-751 24, Uppsala, Sweden

ARTICLE INFO

Article history:
Available online 23 December 2009

Keywords:
Characterization of adsorption processes
Linear methods
Linear solvation energy relationships (LSERs)
Hydrophobic-subtraction method (HSM)
Nonlinear methods
Retention mechanism
Thermodynamic quantities
Adsorption isotherms
Adsorption energy distribution

ABSTRACT

This review discusses nonlinear chromatographic methods of importance for proper characterization of the adsorption processes in analytical chromatographic systems, with focus on reversed-phase liquid chromatography. Linear methods such as the linear solvation energy relationship (LSER) method and the Snyder–Dolan hydrophobic-subtraction model will also be reviewed briefly. The nonlinear methods for adsorption isotherm determination and the tools for further treatment of the nonlinear adsorption data will be extensively treated in a way suitable for the general chromatographer. Applications of the various methods will be given and the outcome and conclusions will be discussed. Special emphasis will be placed on discussing the possibilities of combining linear and nonlinear methods in order to obtain a deeper and more complete investigation of the interactions in the actual phase system.

Contents

* Fax: +46 18 471 3692.
E-mail address: Torgny.Fornstedt@ytbioteknik.uu.se.

0021-9673/$ – see front matter © 2009 Published by Elsevier B.V.
doi:10.1016/j.chroma.2009.12.044

1. Introduction

Separation science is always trying to achieve increasingly better separation performances, but in the past 5–6 years there has been an extraordinary amount of activity in developing new stationary phases and columns for analytical separations. The trends focus mainly on achieving higher sample throughput by improving (i) the column efficiency, (ii) the column permeability or (iii) the stability of the stationary phase material, for harsh conditions such as extreme pH or temperature.

The efficiency trend has a long history. The particle size has been continuously decreased, in order to improve the efficiency, all the way from the 100 μm particles of the fifties to the modern sub-2 μm porous spherical particles of today, via the birth of high performance liquid chromatography (HPLC) in the seventies. The optimum height of one plate (H) is around 2 particle diameters, but with decreasing particle sizes, the backpressure increases inversely proportional to the square of the particle diameter. The flow rate also affects the efficiency. Using the van Deemter curve $H = A + B/u + C \cdot u$ we can estimate a relationship between the linear velocities u ($u = L/t_0$, where t_0 is the column hold-up time) and H. The A-term describes the dispersion (different length of longitudinal flow paths) and the B-term the molecular diffusion, and the C-term is the resistance to mass transfer. Note that the terms are solute-dependent. With decreasing particle sizes the A-term and C-term will decrease due to shorter irregular longitudinal path length and reduced diffusion distance, respectively, leading to higher optimum linear velocity (the linear velocity where H has its lowest value). As example, if the particle size is decreased in an already established method, the method can be operated at a larger linear velocity achieving the same efficiency (and thus maintained R_S) using shorter columns. Reducing the column length will not only increase the speed, but also increase the sensitivity, as the sample zone(s) become(s) less diluted. Because of the limited operational pressure for HPLC (400 bar), the full potential of reduced particle size cannot be utilized. As a consequence the column length has also been decreased with decreasing particle size to operate the separation system within the pressure limit, leading to non-substantial increases in efficiency. Today, up to 1000 bar can be delivered with new commercial so-called ultra performance liquid chromatography (UPLC) systems using sub-2 μm particles.

The permeability trend has also a long historical background which is not, however, as continuous as the efficiency trend. Pellicular material consisting of a solid core covered with a porous shell was first introduced in 1967 [1]. The pellicular material did not become immediately popular because in the early seventies, 10 μm porous silica particles were introduced. However, the interest has now re-appeared, because the low permeability associated with sub-2 μm particles forces the user to invest in UPLC systems. The other advantage of pellicular material is increased mass transfer due to shorter diffusion distances; this effect is manifested in the C-term in the van Deemter equation. Monoliths provide another solution to increase the permeability by increasing the external porosity. Monoliths are single continuous porous materials with through-pores that allow the flow to percolate through and diffusive pores to increase the surface area. Increased permeability allows the user to employ longer columns or increased flow rates [2]. The van Deemter analysis shows that the C-term is smaller due to shorter diffusion distances. However, the A-term is larger, probably because of the large size distribution of the through-pores [3]. Many different monolithic materials have been used, e.g. paper, membranes, silica [4], metal oxides [5] and organic polymers [6]. Chromolith (Merck) was the first commercially available silica rod monolith column with an efficiency comparable to that provided by 5 μm particles, but with a permeability like that of a column packed with 10–15 μm particles.

The new pH-stable silica was first mentioned in the seventies and is actually a hybrid material which consists of a combination of silica and organic polymers [7]. The hybrid materials on the market now use methyl or ethyl groups distributed throughout the particle (Xterra and XBridge from Waters) [8], or surface-grafted ethyl bridges (Gemini from Phenomenex) [9]. The stability is increased because the Si–C bond can withstand hydrolysis much better than the Si–O bond. The Xbridge particles are prepared from tetraethoxysilane and bis(triethoxysilyl)ethane. The column lifetime is reduced at low pH due to acid hydrolysis of the bound alkylsilane. Bulky side groups on the alkylsilane have been shown to shield sterically the bound siloxane from acid hydrolysis [10,11]. Hybrid material and bidentate bound stationary phases also seem to increase the stability [12]. Before the advent of the hybrid material, polymeric and other metal oxide materials were used for separations under alkaline conditions. Both materials have excellent chemical and temperature stability. However, the polymeric materials are less pressure-resistant than silica. Moreover, the efficiency is lower compared to silica columns due to shrinking or swelling of the phases. Metal oxides like zirconia (ZrO_2), aluminina (Al_2O3) and titania (TiO_2) are used in LC. The metal oxides are pressure-stable and have a similar efficiency to that of silica material. However, the popularity of metal oxide is low due to the few commercially available phases, and because silanization chemistry cannot be used for stability reasons [13] and due to a more complex retention mechanism, e.g. ligand exchange on strong Lewis acid sites (around 3–4 μmol/m^2) and anion exchange due to the higher pI of the metal oxides [14]. The silica hybrid material has improved the chemical stability many times over, but only for short-term use. For long-term use under chemically aggressive conditions and at elevated temperatures, only polymeric and metal oxide materials work. High temperature separations are sometimes called green chromatography because less organic modifier or even pure water can be used as an eluent. The reason for this is that the solvent-strength in the eluent increases with increasing temperature; e.g. an increase in the temperature by 4–5 °C approximately equals a reduction of 1% in methanol or acetonitrile [15,16]. Moreover, mass transfer and molecular diffusion increase with the temperature, resulting in a lower C-term but a higher B-term [17].

Among other new stationary phases, hydrophilic interaction liquid chromatography (HILIC) has received great attention [18], probably due to its nearly orthogonal selectivity compared to RPLC [19]. As an eluent, 5–40% aqueous buffer solutions are used in a mixture with acetonitrile; the stationary phase is polar, e.g. pure silica, diols, zwitterions or sugar [18]. HILIC is especially good in separating organic bases, sugar and other polar compounds that are sparingly soluble in the non-polar eluents used in NPLC.

Many new chiral stationary phases (CSPs) have been developed the last decades [20]. Often the CSP comprises of a modified silica support onto which a chiral ligand molecule (so-called selector) has been immobilized. The separation will then be based upon differences in the binding constant between the enantiomers and the particular CSP. Selectors such as large biomolecules (e.g., immobilized proteins) often gives a most convenient phase system for analytical chiral separations; here pH function as a most flexible and predictable tool for adjusting retention times and selectivity. Commonly used proteins are α_1-acidglycoprotein [21], bovine serum albumin [22], α-chymotrypsin [23], cellulase [24] and most recently amyloglucosidase [25]. Protein CSPs are not proper for preparative applications since the loadability is very poor. For preparative purposes cellulose- and amylose-based phases, with trade names Chiralcel and Chiralpak, respectively, has been dominating the last 20 years [26].

This great development of new separation phase systems which has taken place most recently increases the importance of having proper and simple methods for classification of the new systems

and for understanding their putative retention mechanisms. System characterization is also important for increasing the knowledge of the performance of the separation system. The recent guidance for PAT from FDA [27] has increased the interest from the industry in improving their knowledge about the systems. The column can be characterized using material science methods or chromatographic methods; the latter methods can be further classified as linear or semi-linear or thermodynamic and nonlinear. In the linear and semi-linear chromatographic methods we aim at screening the properties of many columns, whereas the latter two methods aim at a deeper understanding of one specific column.

The characterization of modern liquid–solid chromatographic systems assumes most often that adsorption is the underlying retention mechanism, and not partition. In reality, there has been a debate whether the mechanism is adsorption or partition already for more than 30 years ago up to today (see Editor's note in [28]. Adsorption means that a monolayer is formed in which solute or solvent molecules compete to cover the external stationary phase surface. In a partition process, the role of the support is instead to provide the large surface area onto where a stationary liquid phase is deposed. Since late seventies in a pioneer work, and in later numerous papers, it has been demonstrated by equilibrium isotherm measurements that adsorption is the dominant mechanism in reversed-phase alkyl-bonded phase systems, rather than partition. Interestingly, most recent research indicates that the interfacial region between the stationary phase and the bulk liquid can be composed of several layers depending on the character of the organic modifier. The formation of a complex adsorbed four-layer acetonitrile phase was recently confirmed by excess adsorption isotherm data for a modern reversed-phase system [29]. However, the characteristics of the adsorption models and their parameters accounts for these effects and can shed new light on the adsorption mechanism. However, it is recommended that organic modifiers forming less numbers of adsorbed layers are used in experiments aimed at modelling for.

Many linear methods aim at screening columns for the identification of those with different selectivity for method development or for the identification of columns with similar selectivity as backups/replacements. However, most of these aspects are useless unless the column manufacturer can deliver reproducible columns. The LC–GC journal survey showed that this is the single most important factor when selecting a column supplier [30]. The batch-to-batch and column-to-column reproducibility for different solutes' retention times, retention factors, overloaded profiles and adsorption isotherms has been determined on modern silica columns in a series of papers from Guiochon and coworkers [31–35]. The results indicate very high batch-to-batch and column-to-column reproducibility with retention times and retention factors having RSD values around 2–3% and 0.5%, respectively. For overloading studies good peak and adsorption isotherm reproducibility was noted [36,37]. One must stress that the column itself is not the only component responsible for the separation. The characterization method should also describe the role of the mobile phase and temperature in the partitioning process. Even for "isoeluotropic" solvent compositions the selectivity can be altered depending on the selected modifier used in the RPLC eluent. The different physical–chemical properties of the modifiers have been summarized in the so-called "solvation-selection-triangle" [38]. The complexity is even larger for charged compounds where mobile phase effects like chaotropic effects, shielding of charges and ion-paring also should be considered. There are many reasons for energetically heterogeneous partitioning originating from the surface. For example, the solute can interact with silanols (ion-dipole, induced dipole-dipole, etc.) ranging from several hundred kJ/mol to less than 1 kJ/mol in adsorption energy [39]. Other examples involve trace levels of metals leading to increased acidity of residual silanols, interactions between trace metals and chelating agents, homogeneous distribution of ligands on a heterogeneous surface [40,41] and bound-phase forming cavities that are responsible for steric selection [42].

Many different material science methods are used to characterize fundamental surface and bulk properties. Some properties determined are: surface area, pore volume, pore size distribution, particle size distribution, total carbon load and trace metals in the silica matrix [43]. All these properties are useful, but will not be directly related to a chromatographic situation. Nevertheless, material science methods can be very valuable complements to chromatographic methods. Linear characterization is often performed by injecting analytical concentrations of different test solutes to probe different interactions responsible for retention. Usually, the retention factor, the peak asymmetry, and the selectivity of some test solutes are determined. However, often the asymmetry is not included because of the low inter-laboratory reproducibility for this parameter [44]. Some common tests used are referred to as the "Engelhardt" [45], "Tanaka" [46], "Walters" [47] and "Galushko" tests [48]. The problem associated with these types of tests is that the results are not directly comparable because different conditions and solutes are used [49]. Many times columns are clustered using principal component analysis into similar and dissimilar groups, but this approach results in the acquisition of very little physical–chemical information. To obtain more information of this type, a model-based approach like the linear solvation energy relationship (LSER) method can be used. The LSER method is based on describing the bulk properties of the stationary and the mobile phase using linear terms that relate to some interaction. It is a general method that can be used to describe many different systems and operational conditions [50]. However, so far the method cannot properly predict retention and is therefore seldom used for the optimization of separations. A similar model, called the hydrophobic-subtraction method (HSM), has been primarily developed and is primarily used for the characterization and classification of type-B alkyl-silica phases 18 (phases using sol–gel technology); this model usually predicts the retention factor within 2%. Also here linear descriptors are used, but recognized RPLC retention mechanisms such as hydrophobic interaction, steric resistance, ion interaction and hydrogen bond donation and acceptance are used [51]. The models above can at best predict retention times. For a proper peak-shape analysis, a microscopic or macroscopic column model is required [52–55]. Semi-linear characterization is mainly used by McCalley [56]. The method is fast and estimates the columns' saturation capacity by injecting a series of solutions with increasing concentration until the "efficiency" is decreased to at least half. For heterogeneous adsorption processes, the high-energy site at low concentrations is primarily responsible for transforming the peak into a right-angled-triangular peak, and hence the method can only provide a rough saturation capacity for the high-energy site. Thermodynamic characterization is usually conducted by plotting the van't Hoff plot (k vs. $1/T$, where T is the absolute temperature (Kelvin)). The method provides the entropy, enthalpy and Gibbs free energy for transferring a solute from the mobile phase to the stationary phase, assuming temperature-independent entropy. For small solutes, usually the enthalpy is between −10 and −15 kJ/mol [57]. The information can give insights into which kind of interaction is dominant in the partitioning [58]. The limitation is that all the different types of interaction are lumped into one term. Nonlinear characterization is based on determining the adsorption isotherm over a broad concentration range to give a complete investigation of all the interactions – weak as well as strong. There are several thermodynamically valid adsorption models to be fitted to the acquired adsorption data. The Langmuir adsorption isotherm (type I) is the simplest nonlinear adsorption isotherm, describing a finite amount of equal adsorption sites. The bi-Langmuir model

is composed of two different Langmuir terms on the right side of the equality sign and has as example successfully been used to describe the adsorption of enantiomers to protein stationary phases e.g. α_1-acid glycoprotein (AGP) [58]. Other examples of adsorption isotherm models are the Tóth adsorption isotherm, with a unimodal heterogeneous adsorption energy distribution, and the Moreau model, accounting for solute–solute interactions [5,59]. By determining the adsorption isotherm at different temperatures and assembling a van't Hoff plot for each mechanism, mixed sorption mechanisms can be studied and information on each site can be obtained. Another advantage of the use of nonlinear data, instead of linear data, is that an accurately determined adsorption isotherm can directly be used in a macroscopic column model to predict peak profiles for process optimization.

The main purpose of this review is to present the theory and good applications of the most important linear and nonlinear methods for characterization of the adsorption process in analytical separation systems. A relatively larger part of the review will treat the more complicated nonlinear methods where a more complete investigation of all interactions is possible. The review also aims at inspiring the possible combination of linear and nonlinear methods for obtaining an improved knowledge of the adsorption processes.

2. Linear methods used to characterize the adsorption process

2.1. Derivation of thermodynamic quantities in linear chromatography

At equilibrium, the standard Gibbs free energy of adsorption, ΔG°, at temperature T (K) can be written as [59,60]

$$\Delta G = -RT\ \ln K \tag{1}$$

where R is the universal gas constant and K is the thermodynamic equilibrium constant. From classical Gibbs–Helmholtz equation, we can derive the temperature-dependence of the equilibrium constants.

$$\frac{\partial(\ln\ K)}{\partial(1/T)} = -\frac{\Delta H^\circ}{R} \tag{2}$$

This expression, the so-called van't Hoff equation, allows the determination of the standard molar enthalpy of adsorption, ΔH°, from the slope of the temperature-dependence of the logarithm of the equilibrium constant.

The retention factor is the phase ratio F multiplied with the equilibrium constant, i.e. $k = FK$. The phase ratio (F) in turn, is the ratio of the volume solid phase over the volume mobile phase ($F = V_s/V_m$). Since $k = FK$, the lumped equilibrium constant can be easily calculated, if the phase ratio is known, from the relation $K = k/F$. From this relation, a simplified version of the van't Hoff equation is obtained, based on the measurement of the retention factors k at different column temperatures in linear chromatography

$$\ln\ k = -\frac{\Delta H^\circ}{RT} + \frac{\Delta S^\circ}{R} + \ln F \tag{3}$$

The adsorption enthalpy and entropy are derived from the slope, $-\Delta H^\circ/R$, and the intercept, $(\Delta S^\circ/R + \ln F)$, of a plot of $\ln k$ versus $1/T$. This plot is linear if ΔH° and ΔS° do not depend significantly on the temperature within the range used in the measurements, which is the usual case. This approach is generally used in chiral chromatography.

2.2. Linear solvation energy relationships (LSERs)

The solvation parameter model is based on real and defined intermolecular interactions involved in the retention of solutes in equilibrated phase systems and is therefore more useful for a deeper understanding than most linear models. The model is described by a simple equation:

$$\log\ SP = c + eE + sS + aA + bB + vV \tag{4}$$

where SP is a free energy-related property related to the solute, in a similar way to the chromatographic retention factor [61]. Each parameter (so-called solute descriptor) is constructed and included in the LSER equation to account for a specific interaction. The solute's descriptors are the excess molar refractivity (E), the polarity-polarisability (S), the hydrogen-bond donor character (A), the hydrogen-bond acceptor character (B) and the McGowan's molecular volume (V). Retention factors are measured for at least 20 solutes with known descriptors (E, S, A, B and V). Thereafter a multi-linear regression is performed to estimate the coefficients in Eq. (4) (e, s, a, b and v). The values of the coefficients define the solute interactions in the actual phase system. These interactions are charge transfer and π–π interactions (e), dipole-dipole interactions (s), hydrogen-bond interactions (a and b), and dispersive interactions (e and v). The v term also depends on the cavity energy necessary to insert the solute in the actual phase.

The signs and values of the coefficients inform us about the strength and types of the interactions between the solute and the actual phase. For example, a large and positive a term indicates that the stationary phase has strong hydrogen acceptor properties and thus interacts strongly with acidic solutes. If the b term is positive and large, the stationary phase is a strong hydrogen-bond donor and interacts strongly with basic solutes.

2.3. The hydrophobic-subtraction method (HSM)

The solvation parameter model has inspired the development of a new simpler model which is more focused on reversed-phase columns and is called the hydrophobic-subtraction model (HSM). The HSM model assumes that the major contribution of hydrophobicity is first subtracted, so that the remaining sources of contribution to solute retention are better visualized. Five key-parameters are defined to characterize the selectivity and properties of ODS stationary phases; hydrophobicity (H), steric selectivity (S^*), hydrogen-bond acidity (A) and hydrogen-bond basicity (B), and cation-exchange capacity (C).

The equation below relates the logarithm of the retention factor of a compound, relative to ethylbenzene and conditions-independent so-called column parameters (H, S^*, A, B and C) associated with the conditions-dependent so-called solute-column interaction terms (η', σ', β', α' and κ').

$$\log\left(\frac{k}{k_{EB}}\right) = \log(\alpha) = n'H - \sigma'S^* + \beta'A + \alpha'B + \kappa'C \tag{5}$$

where α is a separation factor, k is the retention factor of a given solute and k_{EB} is the retention factor of the non-polar reference compound ethylbenzene (EB) on the same column and under the same conditions [62]. The coefficients η', σ', β', α' and κ' concern certain properties of the solute molecule: hydrophobicity (η'), bulkiness (σ'), hydrogen-bond basicity (β'), hydrogen-bond acidity (α') and effective ionic charge (κ'). These coefficients are relative to values for ethylbenzene, the reference compound for which all the coefficients are zero, and the values of each column parameter (H, S^*, A, B and C) are relative to a hypothetical, average type-B (pure silica) C_{18} column. Any column which behaves identically to this average column will have H equal to 1, and all the other column parameters equal to zero. Therefore, a positive value for a certain parameter indicates an increase in the studied property and conversely, a negative value indicates a decrease in the given property for the studied column. The coefficients are determined by injecting test solutes on a mobile phase consisting of acetonitrile/0.06 M

potassium phosphate buffer 50/50 (v/v); the pH is 2.8, the flow rate 2 mL/min and the column temperature 35 °C.

More particularly, the *H* value increases with an increased ligand density, chain length and degree of end-capping. An increased positive value of the steric selectivity term S^* indicates that the steric resistance is larger for the actual column as compared to the average ODS column, and thus the solute is partly excluded from the bonded-C18 layer. A negative value of S^* indicates that an increase in retention is due to an easier access of the solute to the bonded C_{18} layer. The *A* term is a measure of the proton-donor property of the stationary phase in relation to (proton-accepting) basic solutes. This term decreases with a larger degree of end-capping. The *B* term is a measure of the proton-acceptor property of the stationary phase in relation to (proton-donating) acidic solutes. The degree of end-capping has no effect on the *B* term. Finally, the *C* term is a measure of the ionic interaction capacity of the ionized silanol groups and the term is estimated at both pH 2.8 and pH 7. A high *C* term indicates a high activity of acidic silanol groups.

The linear methods LSERs and HSM do only give values of interest for comparison with other columns useful for the chromatographer in the industry. But it is our hope that these methods in the future will be successfully combined with nonlinear methods for a deeper understanding of the adsorption and retention processes.

3. Nonlinear characterization methods

3.1. Modelling of the chromatographic separation

The nonlinear theory was developed for preparative chromatography and is more complicated than the theory for analytical chromatography. In analytical chromatography, the goal is merely quantitative information, low sample concentrations are injected, and consequently linear conditions prevail. In preparative chromatography the goal is to isolate as much as possible of the desired component(s) in a complex sample mixture and high sample concentrations are injected. Because of the limited surface capacity of the stationary phase, the column will operate under overloaded conditions, and a further increased sample load results in a lower fraction being adsorbed. Thus, nonlinear conditions prevail and the eluted bands of the components at the column outlet are strongly distorted and unsymmetrical. The partition of a substance between the mobile and the stationary phase depends on the local concentration of this compound during the travel in the column. The adsorption isotherm for a certain substance describes the relation between its stationary phase concentration and mobile phase concentration in the actual phase system and at a constant column temperature. The adsorption isotherm provides the essential thermodynamic parameters required for computer simulations. However, the band shape and band broadening are also due to the molecular diffusion and to the slow mass transfer kinetics of the actual component between the two phases.

Recently, modern computing power has enabled the simulation of chromatographic profiles based on complex mathematical models of chromatography [59,60]. Computer modelling of chromatography is important in analytical chromatography because comparisons between experimental results and predictions based on a satisfactory model will tell us to which extent we have understood (i) the operational mechanisms of our separation media and (ii) the thermodynamics and mass transfer kinetics related to an actual separation problem. At fast mass transfer kinetics, the equilibrium-dispersive (ED) model can be used to approximate the migration of molecules through the column [59]. The ED model assumes that adsorption/desorption and mass transfer events are instantaneous, so that the mobile and stationary phases are always in equilibrium. Small deviations are accounted for by the apparent dispersion coefficient, D_a, which lumps together all the dispersive contributions in the column. The ED model is a good choice when separating small solutes with RPLC; such systems are highly efficient with fast mass transfer kinetics. It has been shown that homogeneous kinetic models give nearly identical results to those of the equilibrium-dispersive model if N is larger than a few hundred plates. However, for heterogeneous mass transfer kinetics, the situation is more complicated [63–65]. In the articles covered in this review, the ED models were numerically solved using the Rouchon finite difference scheme [59,60].

3.2. Adsorption isotherms

Depending on the adsorption behaviour, the different types of molecules will elute at different times at the column outlet and pure fractions of respective component are obtained. At a large load of the column, the column will operate under overloaded conditions, because surface capacity of the stationary phase is limited. Thus, at high solute concentrations nonlinear conditions prevail and the eluted bands of the components at the column outlet are strongly distorted and unsymmetrical. Another complication at large sample loads is that the different types of components compete with each other about the same surface, an effect that ultimately results in strong band interactions and band contaminations. The partition of a substance between the mobile and stationary phase thus depends on the local concentration of this compound and the local concentrations of all other compounds. Functions describing the relationship between the compound concentration in the mobile and stationary phases, at a specific and constant temperature (isothermal conditions), are called adsorption isotherms. Several different adsorption isotherm models are available for describing single component as well as n-component systems at constant temperature.

The models can be explicit, i.e. $q_i = f(C_1, C_2, \ldots, C_n)$, or implicit, i.e. $q_i = f(C_1, C_2, \ldots, C_n, q_1, q_2, \ldots, q_n)$. The main problem associated with implicit functions, e.g. the electrostatically modified *n*-Langmuir models [66], is that the calculation of band profiles with the ED model requires the solution of a nonlinear equation in each step, leading to extremely long calculation times [67].

An adsorption isotherm is also classified according to the shape of the isotherm curves [59], see Fig. 1. Most reported liquid–solid adsorption processes are described with type I, Fig. 1a, e.g. as in the Langmuir and Tóth models, but the more complicated type II (Fig. 1b) and type III (Fig. 1c), e.g. as in the Moreau models, have also been reported. In the right-hand column of Fig. 1, the corresponding elution profiles are plotted. Type II and III adsorption isotherms have vertical asymptotes which are not realistic in LC because these adsorption isotherms do not reach saturation at higher concentrations. A type II adsorption isotherm and a type III adsorption isotherm that become saturated at higher concentrations are referred to as type IV and type V, respectively [68]. However, if the solute solubility is low, the saturation at high concentrations cannot be determined. We urge the interested read to read the following literature for a more overreaching view of adsorption in chromatography [59].

The retention time and elution profile of a component are governed by its ability to adsorb to the stationary phase surface and by how it competes with other components. Single component adsorption isotherms describe situations where there is only a single adsorbing solute. The single component Langmuir adsorption isotherm is written as

$$q = \frac{aC}{1 + KC} = \frac{q_S KC}{1 + KC} \tag{6}$$

Here q and C are the stationary and mobile phase concentrations of the solute, a is the distribution coefficient that dictates retention

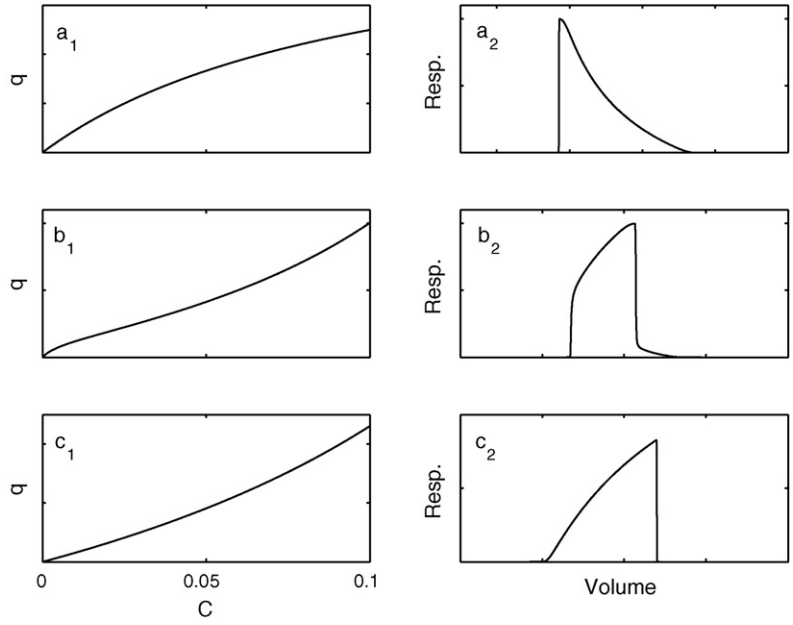

Fig. 1. The left column shows types I, II and III adsorption isotherms and the right column shows their corresponding elution profiles. Reprinted with permission from Jörgen Samuelsson. Copyright Jörgen Samuelsson 2008.

under linear conditions (low concentrations), and K is the association equilibrium constant (not seldom denoted b). The saturation capacity, q_s, describing the maximum adsorbed concentration, can be calculated by the ratio a/K. Thus, the a term is the same as the association equilibrium constant multiplied with the monolayer capacity, $a = q_s K$. The retention time under linear conditions, t_R, becomes

$$t_R = t_0(1 + k) = t_0(1 + FKq_s) = t_0(1 + Fa) \quad (7)$$

where t_0 is the zero hold-up time, k is the retention factor and F the phase ratio (see above). This relation shows how the retention time is governed by the a-term, which can be interpreted as the initial slope of the adsorption isotherm. It can also be seen that the retention time depends on the equilibrium constant and the saturation capacity, which is proportional to the density of the adsorption sites.

The Langmuir model assumes ideal solutions and monolayer adsorption. In many situations the different solutes adsorb to and compete for the same sites. The adsorption is then expressed with competitive models, such as the competitive Langmuir adsorption isotherm:

$$q_i = \frac{a_i C_i}{1 + \sum_i K_i C_i} \quad (8)$$

It is very common that the solutes adsorb to more than one type of site in the stationary phase. This is referred to as heterogeneous adsorption. This is treated semi-empirically by including a second Langmuir term in the model, giving the bi-Langmuir model. Below, the Langmuir model is developed to the bi-Langmuir model:

$$q = \frac{a_I C}{1 + K_I C} + \frac{a_{II} C}{1 + K_{II} C} \quad (9)$$

The model assumes two independent and different types of adsorption sites, often one is chiral and one is non-chiral. The two enantiomers have different affinity for the chiral site but identical adsorption parameters corresponding to the non-chiral site. The model has also been successfully used to describe the adsorption in reversed-phase chromatography; here the adsorption site with the stronger affinity may source from silanol sites [59]. The saturation capacity for each site (q_{sI} respective q_{sII}) describing the maximum adsorbed concentration can be calculated by the ratio a/K for the different sites.

The bi-Langmuir model has successfully been used to describe the adsorption of enantiomers to protein stationary phases, e.g. α_1-acid glycoprotein (AGP). Here, the adsorption process consists of two different types of sites, one enantioselective and one nonselective [58]. The nonselective sites have a large capacity but low adsorption energy, representing many different adsorption sites of similar energy levels all over the surface. The enantioselective sites have a low capacity but high adsorption energy and could be the active site of a protein. The nonselective site is responsible for the overall retention, but decreases the selectivity [69]. The bi-Langmuir model has also successfully been used to describe the adsorption of charged solutes [59] and some uncharged solutes like phenol and caffeine to C18 silica columns [70]. The low capacity site becomes saturated at very low concentrations, which results in a thermodynamic peak tailing as opposed to a kinetic peak tailing. Often, the strong site is blamed for causing bad peak performances, but, on the other hand, in many cases the high-energy site is actually responsible for the selectivity, e.g. chiral phases [71]. Many other single component adsorption isotherms exist that describe other more complicated adsorption processes. Examples are: the Tóth adsorption isotherm, which has a unimodal heterogeneous AED that tails toward lower energy [72], and the Moreau model, which accounts for solute–solute interactions [73].

The models presented above represent only a small selection of the simplest models used for describing (chiral) adsorption to stationary phases. Classically the adsorption models are divided into different types. The most reported liquid–solid adsorption processes are described with type I, Fig. 1a, e.g. the Langmuir and bi-Langmuir models, but the more complicated type II (Fig. 1b) and type III (Fig. 1c) have also been reported. In the right-hand column of Fig. 1, the corresponding elution profiles are plotted. Types II and III adsorption isotherms have vertical asymptotes, which are not realistic in LC because these adsorption isotherms do not reach saturation at higher concentrations.

3.3. Derivation of thermodynamic quantities in nonlinear chromatography

A very important restriction for the simplified van't Hoff equation frequently used in linear chromatography, is that the surface must be homogeneous. This is seldom the case. In most reversed-phase experiments and chiral chromatographic in particular, the adsorption of the various solutes to the chemically bonded phases are best described by heterogeneous models (*cf.* Eq. (9)). In those very common cases, the linear approach does not give a correct estimate of the thermodynamic functions; instead serious errors are introduced interactions as exemplified in [74].

A bi-Langmuir equation (*cf.* Eq. (9)) comprises of two Langmuir term with each one term for the association equilibrium constant for this typical site. The Gibbs–Helmholtz equation is easily adapted to derive the thermodynamic quantities for each adsorption site; so that the individual temperature-dependence of each equilibrium constants is obtained, below exemplified for the case of a bi-Langmuir adsorption model.

$$\frac{\partial(\ln K_{\mathrm{I}})}{\partial(1/T)} = -\frac{\Delta H^{\circ}_{\mathrm{I}}}{R} \tag{10a}$$

$$\frac{\partial(\ln K_{\mathrm{II}})}{\partial(1/T)} = -\frac{\Delta H^{\circ}_{\mathrm{II}}}{R} \tag{10b}$$

The standard molar enthalpy of adsorption for each site, $\Delta H^{\circ}_{\mathrm{I}}$ and $\Delta H^{\circ}_{\mathrm{II}}$ respectively, can be derived from the slope of the temperature-dependence of the logarithm of the equilibrium constant in this equation.

3.4. Methods for determination and evaluation of adsorption isotherms

If the adsorption isotherm is determined over a broad concentration range, it gives information about the strength and capacity of the different adsorption sites in any phase system; the reason is that different adsorption sites dominate at different concentration levels. For example, at a low concentration level, strong but few adsorption sites dominate, while these might be saturated at a higher concentration level where a larger amount of less strong adsorption sites might take over the adsorption. Only by going from low to very high concentration levels, can a complete investigation be made of all the interactions in a phase system. This is to be compared with the information achieved in the traditional way, only measuring the retention times of analytical (Gaussian) peaks. Therefore, the determination of adsorption isotherms and the following treatment and interpenetration of the isotherm data (see below) is of the utmost importance for understanding not only preparative but also analytical separation systems.

3.4.1. Frontal analysis (FA)

Frontal analysis (FA) is usually carried out in a series of programmed concentration steps [59,75]. These experiments can be a series of steps from 0 to C_n, known as the step-series mode, or successive steps from 0 to C_1, then C_1 to C_2, etc., known as the staircase mode. The typical chromatograms for both modes of FA are depicted in Fig. 2.

An integral mass balance is made over the column giving the following equation for the staircase mode:

$$q_{i+1} = q_i + \frac{(C_{i+1} - C_i)\cdot(V_{\mathrm{R},i+1} - V_0)}{V_{\mathrm{a}}}, \tag{11}$$

where C_i and q_i are the solute concentrations in the mobile and the stationary phase after the ith breakthrough. In the step-series mode, q_i and C_i are zero because we always start at concentration zero. $V_{\mathrm{R},i+1}$ is the breakthrough volume, and it can be determined

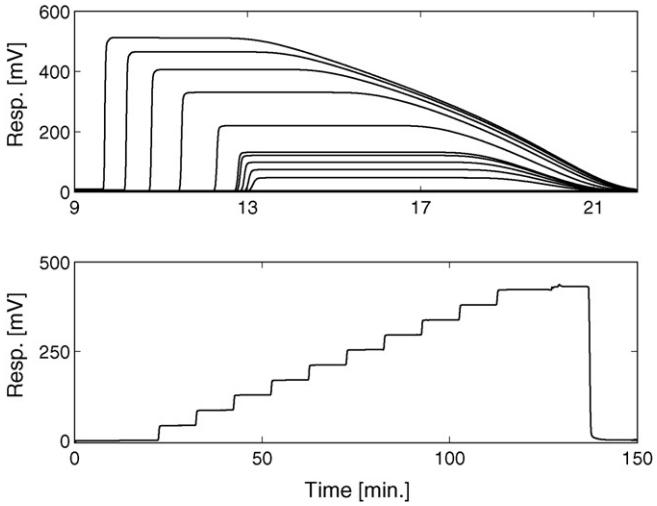

Fig. 2. Frontal analysis for adsorption of methyl mandelate on C18 columns. Top figure some step-series mode and bottom figure staircase mode. Reprinted with permission from Jörgen Samuelsson. Copyright Jörgen Samuelsson 2008.

by: (i) the half-height, (ii) the inflection point and (iii) the centre of mass (i.e. the area) method [76]. The centre of mass method is the only accurate method for the determination of unsymmetrical breakthrough curves. FA is considered to be the most accurate method for the determination of adsorption isotherms and can be used for any type of adsorption isotherm, even at slow and concentration-dependent kinetics [77]. However, for multi-component systems we need to determine the compositions of the intermediate plateaus, which means that a fractionation and reinjection procedure must be followed for systems with more than two components. Unfortunately, it was recently found that high-efficiency columns are required for ternary mixtures, to counteract the erosion of intermediate plateaus by kinetic effects [78].

3.4.2. Pulse methods

The tracer pulse (TP) and the perturbation peak (PP) methods belong to the so-called pulse methods [79–83]. If a small excess of molecules is injected into a column equilibrated with an eluent containing identical solute molecules (a concentration plateau), one single peak will appear in the chromatogram, called the perturbation peak. The injected molecules are eluted in a later eluted and invisible zone. More particularly, a total of three zones are created, one of them being the displaced plateau molecules (i.e. the zone visualized as a peak) and another later eluting zone being the injected molecules (tracer peak). The latter zone will be cancelled out because it has a combined elution with a third zone, the deficiency zone of the plateau molecules, see Fig. 3. This phenomenon was predicted theoretically by Helfferich and Peterson and was called "paradoxical" since it predicted that the same solute would have two different velocities [80]. This "paradox" was later experimentally verified for the first time, by the present authors [83].

Actually the molecules move with one velocity, but as they are introduced they displace some molecules already adsorbed to the stationary phase. The displaced molecules displace other molecules and like a wave crest these are pushed in front of the injected molecules that end up in the wave trough. This is the simplest case, taking place in a one-component system following a type I adsorption isotherm. For a type III adsorption isotherm the TP should instead elute faster than the PP. For type II the retention volumes will be concentration-dependent, see Fig. 4.

The PPs can be used for adsorption isotherm determinations because different concentrations will have different velocities

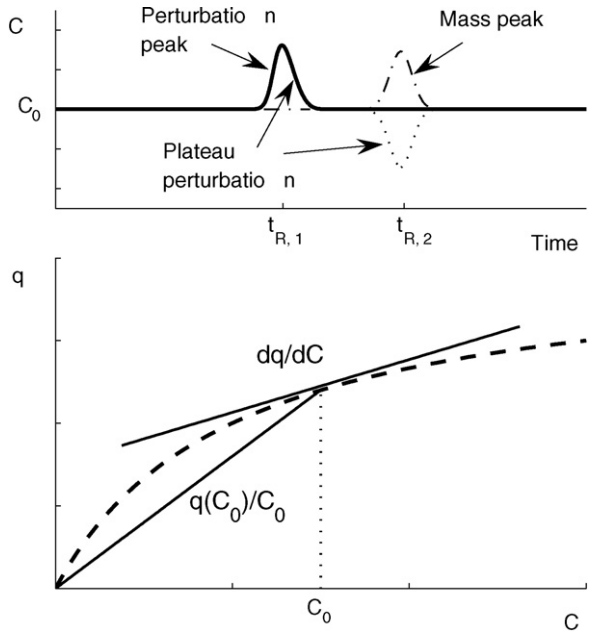

Fig. 3. The figure shows the relationship between the tracer and perturbation peaks assuming a type I adsorption isotherm. The top figure shows a schematic chromatogram, and the bottom one shows a schematic type I adsorption isotherm. The corresponding tangential and cord are associated with the velocity of the perturbation and tracer peak, respectively. Reprinted with permission from [82] © 2006 American chemical society.

related to the tangential slope of the adsorption isotherm at the actual concentration plateau (C_0) [84–86]. The retention volume for a single component perturbation peak is:

$$V_R = V_0 \left(1 + \phi \frac{dq}{dC}\right)\Big|_{C=C_0}, \quad (12)$$

If $C_0 = 0$ and we make an injection of an infinitesimal amount of solute (as in analytical chemistry), we can now express the retention factors with the initial slope of the adsorption isotherms, for the Langmuir adsorption isotherm $k = \phi \cdot a$.

The tracer peak is impossible to detect due to its combined elution with the deficiency zone, unless the sample molecules are labelled somehow (for different labelling methods see [81–83]. The velocity of the tracer peak is governed by the corresponding slope of the chord. The retention volume for a single component tracer peak is:

$$V_R = V_0 \left(1 + \phi \frac{q}{C}\right)\Big|_{C=C_0}. \quad (13)$$

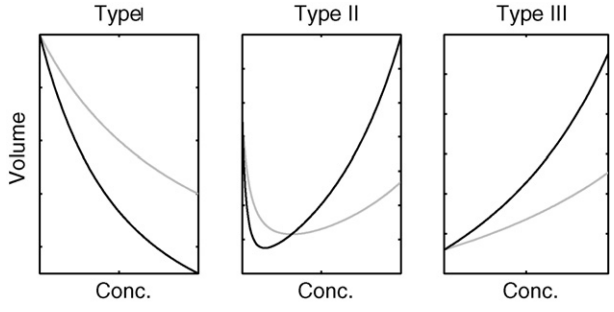

Fig. 4. Retention volumes for perturbation and tracer peaks from type I, type II and type III adsorption isotherms. The grey line is the retention volumes for tracer pulses and the black line for the perturbation peaks. Reprinted with permission from Jörgen Samuelsson. Copyright Jörgen Samuelsson 2008.

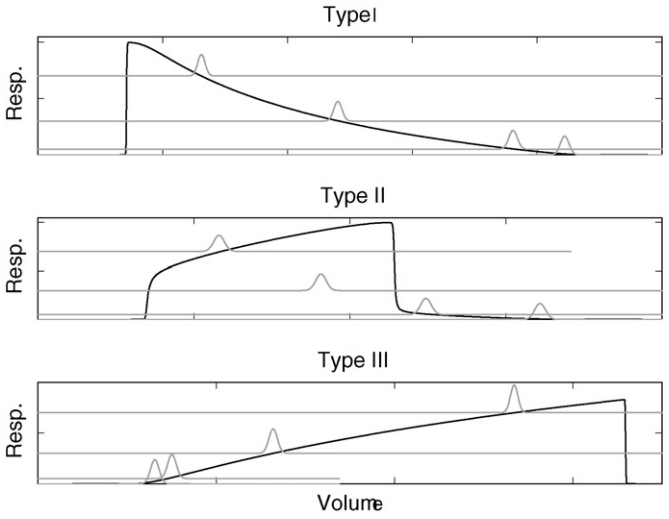

Fig. 5. Overloaded elution profiles originated from a type I, type II and type III adsorption isotherm. The grey lines are the corresponding perturbation peaks. Reprinted with permission from Jörgen Samuelsson. Copyright Jörgen Samuelsson 2008.

3.4.3. Characteristic point methods

It is possible to measure the adsorption isotherm from the diffusive part of a profile. If the diffuse profile comes from an FA step, the method is then called "frontal analysis by the characteristic point method (FACP)", and if it originates from the diffuse part of an overloaded profile, it is called "elution by characteristic points (ECP)" [87,88]. Integrating the diffuse tail of a large overloaded profile for a type I adsorption isotherm we obtain:

$$q(C) = \frac{1}{V_a}\int_0^C (V_R(C) - V_0 - V_{inj})dC, \quad (14)$$

where V_{inj} is the injected volume and $V_R(C)$ is the elution volume corresponding to the mobile phase concentration C. So the ECP method is related to the PP method, but now the slopes are integrated to yield raw adsorption isotherm data. In Fig. 5 overloaded elution profiles and their corresponding PPs at different concentrations are presented for type I, type II and type III isotherms.

From Fig. 5 we further see that in the case of type I and type III adsorption isotherms, the PPs' retention volumes are identical to the corresponding concentration retention volumes for the diffuse part of the overloaded profiles. This is not the case for type II adsorption isotherms, and consequently ECP cannot be used for the acquisition of type II adsorption isotherms.

FACP and ECP are derived using the ideal model and assume infinitely fast mass transfer. This is a rather good approximation for a sufficiently efficient system. Analyses of Langmuir adsorption isotherms and bi-Langmuir adsorption isotherms assuming rectangular injections have shown that for the Langmuir isotherms, $N = 2000$ is required for a minimum error less than 3% [87]. In the case of a bi-Langmuir model, an N of 5000 is required for an error less than 5% [88]. However, the authors considered rectangular injection profiles; this is not the case in an experimental situation. In two recent papers the effect of true injection profiles was experimentally investigated [89,90].

3.4.4. Adsorption energy distribution (AED) calculations

AED calculations provide model-independent information about the numbers of different adsorption sites and their respective energy levels. AED calculations have therefore become a very important tool prior to the selection of an adsorption isotherm

model, helping to narrow down the number of possible rival models, which is why the following theoretical background is important in this context. The Langmuir adsorption isotherm model can be extended to a continuous distribution of independent homogeneous sites across a certain range of adsorption energies.

$$q(C) = \int_{K_{min}}^{K_{max}} f(\ln\ K)\theta(C, K)d\ln K, \quad (15)$$

where $\theta(C, K)$ is the local adsorption model (usually the Langmuir or Jovanovic model is used, but BET has also been used as a local model [91]) and $f(\ln K)$ is the AED. K_{min} and K_{max} are governed by $1/C_{max}$ and $1/C_{min}$, respectively, where C_{min} and C_{max} are the lowest and highest mobile phase concentrations, respectively, measured in the adsorption isotherm [92,93]. The AED can be solved by many different methods [94]. One method is the expectation maximization method [95], where the integral equation is discretized to a sum and solved in an iterative manner. We will see (below) that the calculation of the AED is an important step in the adsorption isotherm model discrimination process.

In a recent study, the AED calculations are expanded to include tangential slope data of an adsorption isotherm generated by the perturbation peak (PP) method, so-called raw slope data (dq/dC) [96]. However, it is important to remember that the AED-tool also has limitations, as example the proper number of iterations must be selected and a high surface coverage is necessary for proper calculations of high capacity sites (see below). When the AED calculations are used properly, to tell which models are realistic and which are not, it is an excellent tool that should always be included before the fitting procedures.

3.5. Measurement of reliable equilibrium data

Before measurements of equilibrium data, we need to have a brief understanding of the "role" of the ingredients in the system. As example, some mobile phase compounds (additives) need to be treated as extra components, e.g. TEA, because it has a strong adsorption to the stationary phase, while some other components are not involved in the partitioning process instead they modify the polarity [97,98]. Describing adsorption for an amine using TEA as an additive with a single component adsorption isotherm is not correct, and misleading conclusions may be drawn from such an approach. Another aspect is that, when we investigate the adsorption of protolytic solutes, we must ensure that the pH is stable so that the ratios of charged and uncharged forms are constant and dependent on the solute concentration. Even a minor pH-shift can lead to dramatic changes in the retention mechanisms. Both these examples will lead to serious errors in the interpretation of the adsorption mechanism.

3.5.1. Experimental and method considerations

Several factors need to be considered during characterization, including those related to the solute, eluent, system or method. Before we choose a method for determining the adsorption isotherm, we need to know if the kinetic contributions can be neglected or not. If our separation system is described with concentration-dependent kinetics or slow mass transfer, especially heterogeneous kinetics, several methods for adsorption isotherm acquisition cannot be used without losing accuracy in the adsorption isotherm data. Especially, the ECP and FACP methods are sensitive to even slight deviations from the ideal model. Usually this is not a problem when separating small solutes using modern stationary phases described in the introduction of this review. The range and density of the data points are another important aspect. The adsorption isotherm determination requires a broad range of concentration data; this is especially crucial for heterogeneous adsorption isotherms. The low concentration data are used to investigate the distribution coefficients, the medium concentration range is used for deducing the high-energy sites, and finally the high concentration data are needed to determine the low-energy sites. For adsorption isotherms containing inflection point(s), the collected data set should also cover this (these) concentration(s). Götmar tried to fit a Langmuir model for raw data which originated from a bi-Langmuir model that covered low to high concentrations [99]. The Langmuir model fitted very badly, but by removing the high concentration data, the Langmuir model fitted excellently. This shows that too narrow a concentration interval may result in the assumption that the wrong model is being used. The use of too narrow concentration ranges with only low concentration data is rather common in the literature, especially in biochemical applications [100,101]. Often, and not surprisingly, homogeneous adsorption processes give a good description of this data set. Even worse is that several times chiral drugs are investigated (in SPR) without specifying which enantiomer is being used [102]. Extrapolating adsorption data is always dangerous. In another study the importance of low and high concentration regions for a system described by a bi-Langmuir model was experimentally investigated [103]. It was found that the bi-Langmuir model could be fitted well to adsorption data if the surface coverage was at least 40% and that coverage of up to 70% was needed for AED calculations. Missing low concentration data points lead to larger error in the high-energy site, and high-energy AED sites may also be unresolved [103]. The data density was also investigated. It was also recently demonstrated that a too narrow concentration range also can lead to misleading conclusions using other technologies for binding measurements such as a modern biosensors, based on surface Plasmon resonance technology [104].

It is concluded that there is no significant effect if as few as 8 data points on the adsorption isotherm parameters are noted, if and only if the data points cover all the interesting concentration ranges [103]. However, this is impossible to know before the adsorption isotherm acquisition, and the required data point density is also very dependent on the complexity of the adsorption process, as mentioned above.

An error in the hold-up time (or the total column porosity) will affect the adsorption isotherm parameters and, in the worst case scenario, will also lead to the assumption of the wrong adsorption mechanism [105]. For a separation described by the Langmuir model, an underestimated hold-up time may lead to the assumption of a more heterogeneous model and an overestimated hold-up time may result in the suggestion of different adsorption mechanisms, like solute–solute interactions (the Moreau model) or multilayer adsorption (BET) [105,106].

Finally, control of the temperature is essential if isothermal parameters are to be measured. Experimentally this could be achieved by using water baths. The temperature effect on the equilibrium constant can be estimated using the van't Hoff relationship and Eq. (4). Sample-eluent mismatch is another source for errors. The reasons for sample-eluent mismatch during characterization studies are numerous; e.g. the sample may have been dissolved in a different solvent for increased solubility, the organic portion may have evaporated differently in the eluent compared to the sample, and dissolved solute may have caused changes in the pH or viscosity. If there is a difference in the viscosity between the samples and the eluent, the sample band in the column may suffer from hydrodynamic instability. The instability can give rise to a "fingering" structure as the low viscous solution fingers into a high viscous solution, thereby deforming the peak [107–110]. Most recently, irregular elution behaviour has been observed in reversed-phase HPLC even at low viscosity contrasts, insufficient to initiate viscous fingering [111,112]. In this context it is also important to mention that a solvent-strength mismatch between the sample and

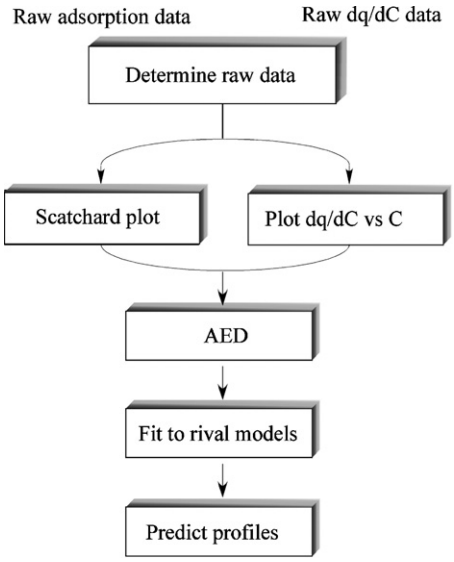

Fig. 6. Flow sheet of the adsorption isotherm selection procedures for raw data.

eluent could lead to peak distortion or even multiple peak-split [113,114].

3.5.2. Adsorption isotherm model selection

Traditionally, adsorption isotherm models have more or less been selected only based on fitting to a preferred model. The preferred model has most commonly been the simple Langmuir model, and rival models have seldom been tested. More recently, a more stringent methodology has been proposed consisting of several steps for analyzing the raw data before the final model selection. Having a correct model is not necessarily a requirement when we are interested in predicting profiles for optimizing processes; if that is the case, we choose a model which is as simple as possible and at the same time can give a good prediction. However, if our interest is to understand the chromatographic process, we need to choose models that better describe the true physical interactions. In this section, you will be guided through a more rigorous method for deciding which model is best for describing the system. The method is presented as a flow sheet in Fig. 6.

Firstly, the adsorption isotherms are categorized as to the type of adsorption isotherm by visual inspection of overloaded peaks, see Fig. 1. If we know the type of adsorption isotherm, we can select a suitable adsorption isotherm determination method (see Section 2.3). We distinguish between raw adsorption isotherm data (actual points on the adsorption isotherm) and raw slope data (dq/dC) derived from the PP method. After the adsorption isotherm determination, raw adsorption isotherm data are plotted as a Scatchard plot (i.e. q/C is plotted vs. q); the curvature in a Scatchard plot indicates the adsorption process, see Fig. 7. A linear Scatchard plot is

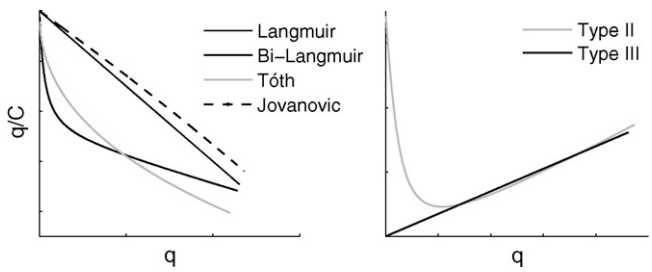

Fig. 7. Scatchard plots for Langmuir, Tóth, bi-Langmuir, Jovanovic and Moreau in (a) and in (b) for type II and type III are plotted. Reprinted with permission from Jörgen Samuelsson. Copyright Jörgen Samuelsson 2008.

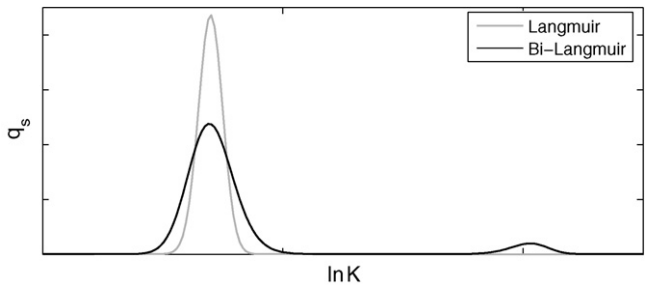

Fig. 8. Adsorption energy distribution for Langmuir and bi-Langmuir models. Reprinted with permission from Jörgen Samuelsson. Copyright Jörgen Samuelsson 2008.

only true for the Langmuir model and has classically been used to estimate the adsorption isotherm parameters; here the lines' intercept with the q/C axis gives the a-value and the negative slope is the K-value. A concave Scatchard plot is true for e.g. Tóth and n-Langmuir models, and a convex plot is true for e.g. Moreau and Jovanovic models. Even more complicated Scatchard plots are found for adsorption isotherms containing inflection points.

The third step is to calculate the AED. This step is most straightforward for the type I adsorption isotherm, but has also been carried out for type II adsorption isotherms [96]. The purpose is to be able to distinguish between heterogeneous and homogeneous adsorption models, see Fig. 8. The method has only been used for raw adsorption isotherm data, but a very recent publication shows that Eq. (12) can also be expanded to handle PP data [96].

The fourth step involves the actual fitting of models to raw adsorption isotherm data or slope data. The previous step has hopefully narrowed down the number of possible models to only a few. Observe that, after the fitting, the raw data are presented as "parameter estimation", because we have biased the data by "assuming" a model. After the fitting, the Fisher parameters are calculated for all the models.

$$Fisher = \frac{(n-l)\sum(q_i-\bar{q})^2}{(n-1)\sum(q_i-q_{\text{fit}})^2}, \tag{16}$$

where q_{fit} is the stationary phase concentration predicted with the model, l is the number of adjustable parameters in the model, and q is the average stationary phase concentration value. By taking the ratio of two Fisher parameters and comparing the value against critical F-test values, one can deduce which model is significantly better in describing the system. The demand for the Fisher parameter to be valid is that the residuals should be normally distributed; this could be tested by plotting normal plots. As always, we need to inspect if the estimated adsorption isotherm parameters are physically reasonable. Finally, the model is used to predict profiles. This can be accomplished by comparing the overlap between the simulated and the calculated profiles [115,116]. The overlap is defined as:

$$Overlap = \frac{\int_0^\infty \min[C_{\text{sim}}(t), C_{\text{exp}}(t)]dt}{\int_0^\infty C_{\text{sim}}(t)dt}, \tag{17}$$

where C_{sim} and C_{exp} are simulated and calculated chromatograms, respectively. The advantage of this expression, as compared to the least-square comparison of twp profiles, is that the chromatographer obtains a number which relates directly to the degree of overlap. If the overlap is 100%, the profiles co-elute, and if the overlap is zero, the profiles do not co-elute at all.

3.6. Applications on analytical chromatographic systems

3.6.1. Linear characterization

Values of the column parameters (H, S^*, A, B, C) have now been measured for more than 399 reversed-phase columns, according to a rather recent review of the HSM method [117]; this allows quantitative comparisons of column selectivity. This is of practical importance concerning the selection of columns with regard to (i) equivalent properties for replacement or (ii) very different selectivity for resolving previously overlapping peaks. Successful examples of column selection for several previously developed routine reversed-phase separations are summarized in a recent HSM review. The use of following formula is used to weight the importance of the column specific parameters in controlling selectivity in to one comparative value to determine if the two columns are equivalent or not [118]:

$$F_S = \{[12.5(H_2 - H_1)]^2 + [100(S_2 - S_1)]^2 + [30(A_2 + A_1)]^2 + [143(B_2 - B_1)]^2 + [83(C_2 - C_1)^2]\}^{1/2} \quad (18)$$

The equation is used to weight the column specific parameters into one comparative value, and determine if the two columns are equivalent or not: columns with a value of $F_S < 3$ are likely to provide equivalent selectivity ($R_S < 2.0$) and separation for different samples and conditions. A value of $F_S \leq 10$ suggest that the two columns are similar enough for the separation of many compounds [119,120].

More interesting in the context of this review is the fact that the values of the solute-interaction coefficients and column parameters are consistent with the physical–chemical understanding of the interactions represented by each of the column parameter terms.

Recently, 371 reversed-phase columns were characterized based on the five column parameter interaction terms [120]. The study focused on the use of the data for interpenetrating peak tailing and column stability. An 18 solute procedure was used and the mobile phase was a 50% acetontrile/pH 2.8 buffers; the temperature was 35 °C and the flow rate was 2.0 mL/min. Among other results, it was found that older type-A alkyl-bonded columns can be differentiated with a 95% certainty from more recent, less acidic type-B columns, by the column parameters B and C. Type-B columns show excellent peak symmetry for the separation of basic compounds at low pH, while many type-A columns show significant peak tailing. For basic solutes separated on type-A columns, the degree of peak tailing tends to increase for larger values of C-2.8. It has also been shown that a shorter 10-solute procedure is as accurate as the 18-solute method, but only for type-B silica columns [119].

Eq. (18) has been tested for 150 solutes of widely different molecular structure and for several hundred reversed-phase columns including C1-30 alkyl-silica columns, embedded polar group columns, polar-end-capped columns, cyano columns and most other commonly used column types.

In a most recent paper, the HSM was used for prediction of column orthogonality of neutral compounds [121]; such compounds are much more difficult to resolve than resolving protolytic ones that can be ionized at different degrees depending on the mobile phase pH. The authors aimed at developing guidelines how to use the HSM to find columns, when two compounds having a combined eluting on a primary column should be resolved. For ionized solutes the Fs-parameter should be used to predict orthogonality while for neutral compounds the cation-exchange term should be dropped, that means $[F_s(-C]$. For the case when the sample contains both ionized and neutral components, F_s and $[F_s(-C]$ should be combined. The proposed procedure was successfully validated by involving 64 neutral compounds and columns from a 400-column database.

3.6.2. Nonlinear methods

3.6.2.1. AED calculations using slope data. The calculation of the adsorption energy distribution (AED) is a recent development that has made a big difference, and it was introduced as an important tool for the chromatographic community for the characterization of modern phases. The reason is that AED calculations provide model-independent information about the numbers of different adsorption sites and their respective energy-levels, prior to the selection of an adsorption isotherm model, which narrows down the number of possible rival models (*cf.* Fig. 6). The selection of a proper model for the fitting of the determined raw data is crucial; if the wrong model is selected, misleading information about the retention mechanism may be deduced.

The drawback with AED calculations is that they require raw adsorption isotherm data (i.e. data points), which unfortunately cannot be obtained by all isotherm determination methods, including the newly validated perturbation peak method. Therefore, recently a mathematical expression was developed allowing the use of the raw tangential slope provided by the perturbation peak method for AED calculations [96]. The approach worked excellently and was verified against both computer-generated adsorption isotherm data and experimentally determined data, using three different experimental systems. It was found that the calculations of the AED based on perturbation peak data convert faster and are not more sensitive to experimental noise as compared to classical AED calculations using raw adsorption isotherm data.

When the AED calculations were adapted for PP data, FA data were used as a reference [96]. The model compounds used were the neutral compound methyl mandelate (MM) and propranolol hydrochloride (PR). The eluent for the MM-system was 30/70 (v/v) methanol/water and that for the PR-system was 45/55 (v/v) methanol/60 mM acetate buffer (pH 4.74 in the pure buffer and measured to 5.46 in the eluent). Fig. 9 shows the AED calculated from PP and FA raw data, respectively; the PP and FA data give approximately the same adsorption energy, and the energy distribution is narrower for the PP data as compared to the FA data. MM has a unimodal AED and a linear Scatchard plot, which strongly indicates that the adsorption process is described by a Langmuir model. The Langmuir model fitted both the PP and the FA data. For PR the Scatchard plot is concave, indicating a bi-Langmuir adsorption (*cf.* Fig. 7), and the AED has at least one unresolved site at low

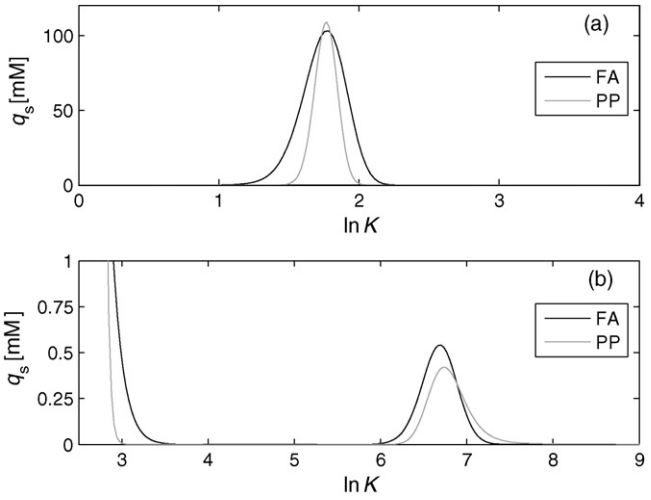

Fig. 9. AED calculated from experimental frontal analysis data and perturbation peak data, respectively, using 1 million iterations and 350 grids points. (a) Methyl mandelate and (b) propranolol, the grey line represents PP and the black line FA data. The calculated results are presented in Table 1. Reprinted from Ref. [96], Copyright 2008, with permission from Elsevier.

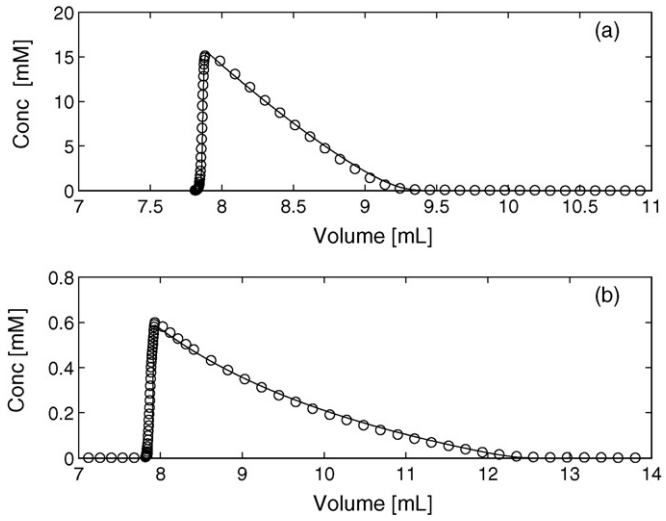

Fig. 10. Simulated and experimental profiles are plotted for 100 μL injections of (a) 100 mM methylmandelate and (b) 10 mM propranolol. The symbols are experimental data and the lines are simulated data using the adsorption isotherm determined with the perturbation peak method. Reprinted from Ref. [96], Copyright 2008, with permission from Elsevier.

energy and one resolved site at high energy (*cf.* Fig. 9). The unresolved site is due to the fact that the concentration used in this determination is not high enough to resolve the high-energy site; a total of 17% of the surface coverage for site 1 is not enough to resolve this site [94–96]. However, the AED shows that the adsorption isotherm used should at least have a bimodal AED. There are many models describing bimodal distributions, such as the bi-Tóth and bi-Langmuir models. The present authors made a statistical evaluation of the rival models describing the bimodal distributions of PR. The adsorption data fitted the bi-Langmuir model well, and no significant (based on the *F*-test 95%) improvement was noted for the electrostatically modified bi-Langmuir or bi-Tóth models. This strongly indicates that the adsorption isotherm of the bimodal distribution of the AED of propranolol is a bi-Langmuir model. Previously, Gritti and Guiochon also found that the PR partitioning is described best with the bi-Langmuir model on a Kromasil C18 column using 60:40 (v/v) methanol:acetate buffer (pH 4.75 in the aqueous buffer) [122].

Finally, the selected models for MM and PR are used to simulate elution peaks and these are compared with experimental chromatograms, see Fig. 10. The chromatogram from a 100 μL injection of 100 mM MM is presented in Fig. 10a, where the solid lines are the simulated profiles and the open circles are experimental data. The simulated profile and experimental profile nearly totally co-elute, indicating a very good model agreement. To obtain a quantitative value for this co-elution, the overlap was calculated and is presented in Table 1. For MM the overlap is very good, with 95% and 98% for adsorption isotherms determined with the FA and PP method assuming the Langmuir model, respectively. The AED calculations also gave an estimated adsorption isotherm which was also used to predict models and the overlap was also excellent here, with around 95% overlap for both data sets used in the AED calculation (*cf.* Table 1).

This indicates that the adsorption of MM is convincingly described by the simple Langmuir model. The adsorption of PR is best described with the bi-Langmuir model, where the second site is around 50 times stronger and has around 4% of the total capacity compared with the first site. To summarize, the AED method was expanded so that the slope of the adsorption isotherm could also be used, i.e. data provided by the perturbation peak method [96].

3.6.2.2. Characterization of reversed-phase systems. There are innumerable commercial reversed-phase columns in the market, and up to today this type of column represents the mode of chromatography most used in the industry. Consequently, as described above in the section on linear methods, there is a need for proper classification and characterization of these columns. By also using nonlinear methods and measuring the adsorption isotherms of model compounds and evaluating their Scatchard and AED-plots, the surface heterogeneity of the columns can be determined. By surface heterogeneity, we mean the different possible sources of heterogeneity in adsorption between the solute and the stationary phase. This requires heterogeneity both of the stationary phase and of the sample molecule. The stationary phase can be heterogeneous due to the complex architecture of the adsorbent and the possible presence of residual silanol groups. The "chemical heterogeneity" of the sample molecule can, for example, consist of a charged or a non-charged polar head and a larger hydrophobic part.

In one recent study by Gritti and Guiochon, the adsorption of caffeine was studied on two C_{18}-bonded phases, one end-capped (XTerra-C_{18}) and one non-end-capped (Resolve-C_{18}), using the experimental procedure described above [123]. More specifically, firstly the adsorption isotherms were determined by frontal analysis (FA). A total of 32 data points were acquired in a concentration range between 0.001 and 24 g/L, e.g. a dynamic range of 24,000. Thereafter, the adsorption data were analyzed with AED calculations. The AED calculations showed clearly the bimodal and quadrimodal distributions for XTerra-C18 and Resolve-C18, respectively. The best adsorption isotherm models were the bi-Langmuir and the tetra-Langmuir isotherms for XTerra and Resolve, respectively. The experimental adsorption isotherms of caffeine for Resolve and XTerra are given in Figs. 11a and 12a, respectively. The symbols correspond to the FA data points and the solid lines to the best isotherm model. The corresponding AED-plots show clearly that there are four types of adsorption sites using the Resolve column (Fig. 11b) and only two types of adsorption sites using the end-capped XTerra column (Fig. 12b). The AED-plot of the interactions with the Resolve phase shows further that the interaction

Table 1
The table shows the adsorption isotherm parameters determined with different methods. The overlap is calculated as the area overlap compared with experimental 100-μL injection of 100 mM for methyl mandelate and 10 mM for propranolol.

Solute	Method	Site 1		Site 2		Overlap [%]
		q_s [M]	K [1/M]	q_s [mM]	K [1/M]	
Methyl mandelate	PP	1.33	5.84	–	–	98
	FA	1.32	5.93	–	–	95
	AED-PP	1.33	5.87	–	–	94
	AED-FA	1.35	5.96	–	–	95
Propranolol	PP	0.208	17.3	6.12	1110	92
	FA	0.176	20.4	6.81	1006	98
	AED-PP	NA	NA	7.28	1079	NA
	AED-FA	NA	NA	8.60	815.1	NA

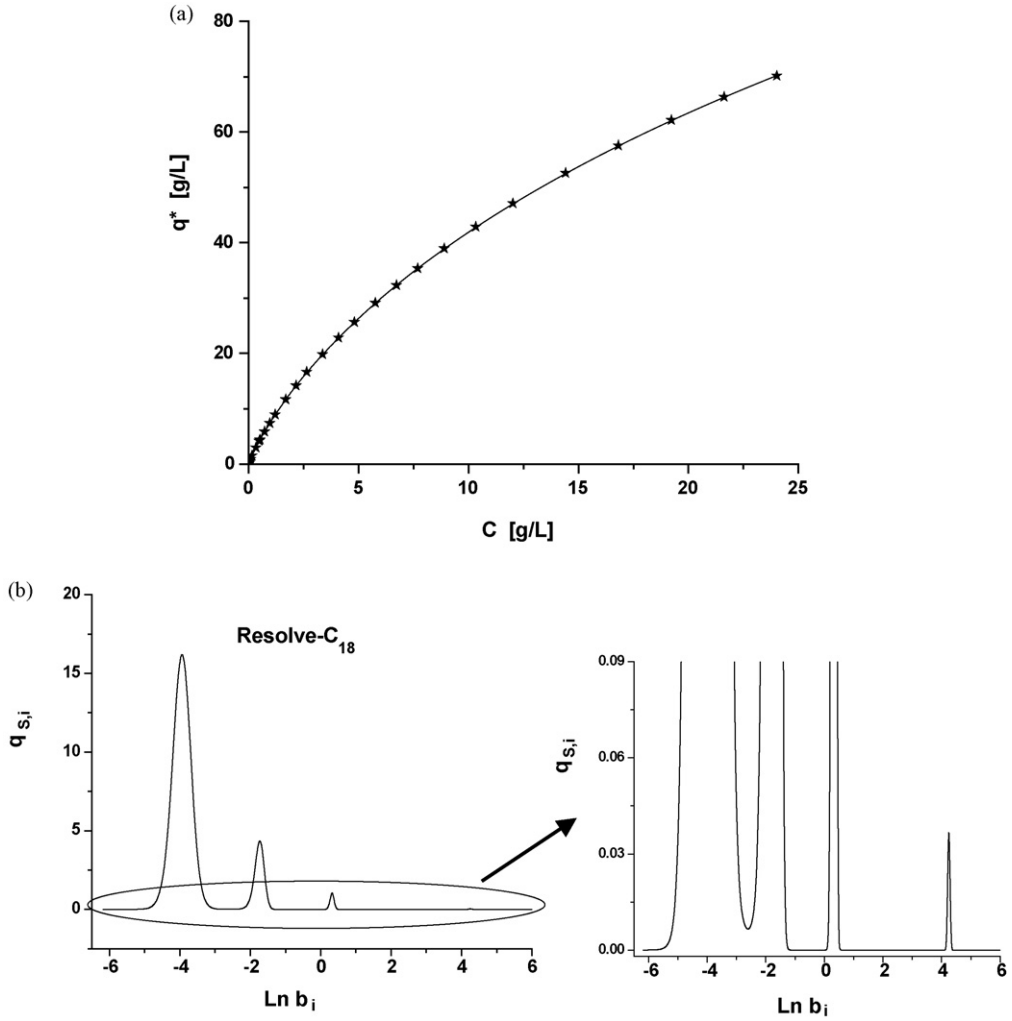

Fig. 11. (a) Adsorption isotherm data of caffeine on Resolve-C18 (full stars) and best isotherm fitting using a tetra-Langmuir isotherm (solid line). Mobile phase methanol/water (25/75, v/v), T = 296 K. (b) Adsorption energy distribution calculated from the raw experimental data (top graph). Note the existence of four adsorption sites. Reprinted with permission from [123]. Copyright 2005 American Chemical Society.

energy of the sites is decreased considerably from the right-hand side to the left-hand side of the AED-plot; i.e. from around ln b 4 to around ln b-4, which constitutes an almost 3000-fold difference (remember that b is the same as term as is denoted K in Eqs. (6)–(9)). A most interesting feature in this context is that the Henry constants ($a_i = q_{s,i} \times b_i$) for each of the four sites are of equal sizes; they are 2.9, 3.8, 3.2 and 3.9, respectively, for types 1, 2, 3 and 4 of the tetra-Langmuir isotherm. Thus, none of the contributions of each of these types of sites can be considered as negligible compared to those of the other ones, despite the drastic decrease in interaction energy going from the left-hand side to the right-hand side of the AED-plot in Fig. 11b. The reason is, of course, that the number of adsorption sites (the capacity of the sites) increased in the opposite direction as the energy decreased. This is visualized by the great increases of the areas of the AED-plots when going from high-energy sites on the right to the low-energy sites on the left.

The presence of a low density of high-energy adsorption sites on Resolve-C_{18} caused retention times and column performance to decrease in a range of sample size that was 100 times lower as compared to XTerra-C_{18}. The experimental chromatograms agreed closely with the band profiles calculated using the best isotherm parameters, which further validated our adsorption model.

In another study, the same authors measured adsorption isotherms of caffeine and phenol, as model compounds, on six different commercial brands of end-capped C_{18}-bonded silica columns [124]. Five of these were monomeric bonded phases: Kromasil, Waters Symmetry, Phenomenex, Hypersil, and Chromolith from Merck; one column was a polymeric bonded phase, Vydac. Adsorption isotherms were acquired by frontal analysis (FA) for these columns in the same way and using a large concentration range and density in 22 data points of the model compounds phenol and caffeine. Scatchard plots and AED-plots were calculated based on the adsorption isotherm data. The Scatchard plots all have concave shapes typical of bi-Langmuir models (*cf.* Fig. 7). The AED-plots revealed that the adsorption energy was bimodal for both compounds on the six different C_{18}-bonded silica surfaces. Therefore, the adsorption isotherms could all be modelled using a bi-Langmuir isotherm model. The bi-Langmuir models consisted of one Henry constant (a term) for each site, a_1 and a_2. This is the same as the slope of the initial part of the adsorption isotherm. The Henry constant is the same as the equilibrium constant per unit volume, which is the information gained from retention factors of linear data ($a = 1/F$). However, by only using nonlinear data, it is not possible to distinguish the Henry constants of site 1 and 2, respectively. Moreover, the bi-Langmuir model also gives the adsorption strength of each site, i.e. the energy of interaction per site (b_1 and b_2), as well as the monolayer capacity of each adsorption site ($q_{s,1}$ and $q_{s,2}$). In fact, the number of adsorption sites (q_s) multiplied by

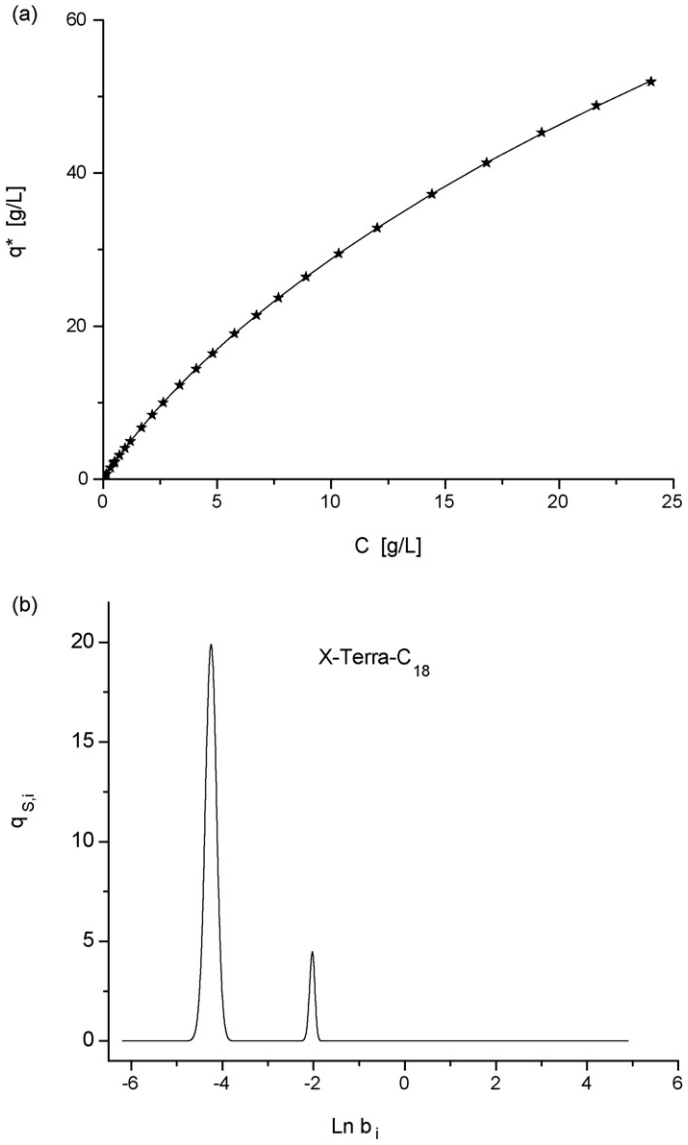

Fig. 12. (a) Adsorption isotherm data of caffeine on XTerra-C18 (full stars) and best isotherm fitting using a bi-Langmuir isotherm (solid line). Mobile phase methanol/water (25/75, v/v), T = 296 K. (b) Adsorption energy distribution calculated from the raw experimental data (top graph). Note the existence of two adsorption sites, only, similar to the first two observed with the Resolve-C18 adsorbent. Reprinted with permission from [123]. Copyright 2005 American Chemical Society.

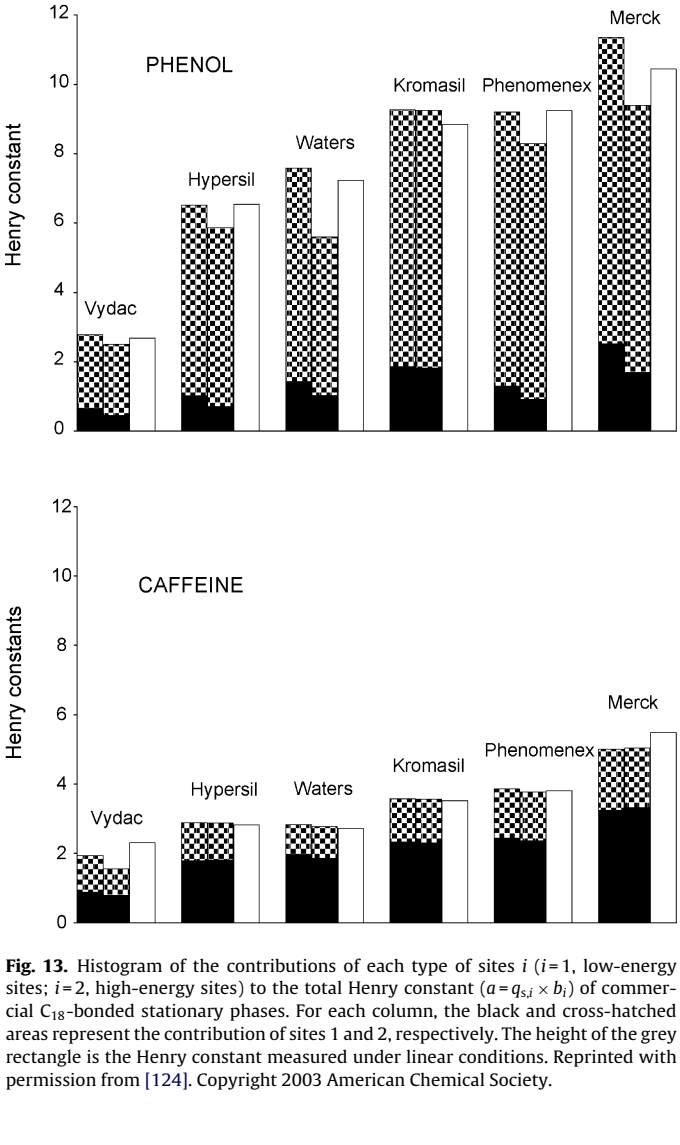

Fig. 13. Histogram of the contributions of each type of sites i (i = 1, low-energy sites; i = 2, high-energy sites) to the total Henry constant ($a = q_{s,i} \times b_i$) of commercial C_{18}-bonded stationary phases. For each column, the black and cross-hatched areas represent the contribution of sites 1 and 2, respectively. The height of the grey rectangle is the Henry constant measured under linear conditions. Reprinted with permission from [124]. Copyright 2003 American Chemical Society.

the energy of interaction per site (q_s) gives the adsorption constant per unit volume, i.e. $a_i = q_{s,i} \times b_i$. Consequently, by evaluation not only of the Henry constants but also of the parameters that compose the Henry constants, a closer understanding of the adsorption behaviour of phase systems is possible. Such parameters (a_i, b_i and $q_{s,i}$) are obtained both from the fitting of the bi-Langmuir model to the adsorption isotherms and from the AED calculations.

Fig. 13 shows a comparison of the contributions of the high- and low-energy sites, 1 and 2, to the linear retention of the two compounds for each column. This is a histogram where, for each column, the rectangles representing Henry constants calculated in different ways are plotted together. The rectangle on the left-hand side shows the Henry constant as derived from the fitting of the adsorption data to the bi-Langmuir model ($a_1 + a_2$), the middle one the Henry constant obtained directly from the AED calculations and the one on the right-hand side the Henry constant obtained from the linear experimental data. In the first two cases, the contributions of each site (a_1 and a_2) can be measured separately, and are represented in the rectangle as black (site 1) and cross-hatched (site 2) areas. The whole of the right-hand rectangle is grey, since in this case only the global Henry constant can be measured. Site 1 is the low-energy site and site 2 the high-energy site ($b_1 < b_1$). Consequently, site 1 has a higher capacity than site 2 ($qs_1 > qs_2$). The linear data (grey, right-hand rectangles) showed that phenol is retained almost twice as much as caffeine on the five "monomeric" columns, while caffeine is almost retained as much as phenol on the "polymeric" Vydac column. The low retention of caffeine relative to phenol is paradoxical, since (i) the molecular weight of caffeine (M_w = 194.2) is more than twice that of phenol (M_w = 95.1) and since (ii) the solubility of phenol ($\geq$6 mol/L) is more than 5 times higher than that of caffeine ($\leq$0.2 mol/L). Therefore, this difference, observed from linear data, is not due to sample hydrophobicity or solubility. However, a closer look at the rectangles in Fig. 13 makes it clear why caffeine is retained less than phenol; the contribution of the high-energy sites (site 2, cross-hatched areas) to the retention of caffeine is much smaller than their contribution to that of phenol. However, the retention contribution of the low-energy sites (site 1, black areas) is larger for caffeine as compared to phenol, and the sources of interaction for this more general site are probably based on such general properties as hydrophobicity and solubility. Upon a closer look at the b and qs terms, it could be concluded that the reason for the larger contribution of the nonselective site 1 is that the b_1 terms of caffeine were much larger, while its capacity

terms (qs_1) were smaller as compared to phenol. For example, for Phenomenex the b_1 term for caffeine is 2.57 L/mol as compared to 0.945 L/mol for phenol, while the qs_1 term for caffeine is 0.95 mol/L and that for phenol 1.371 mol/L. The smaller capacity terms of site 1 for caffeine are logically of the same size as the difference in the molecular size between phenol and caffeine. The larger b_1 values of caffeine reflected larger degrees of hydrophobic interactions. Altogether the capacity and the energy of interaction of site 1 ended up with a larger retention contribution, i.e. a larger Henry constant a ($a = b \times q_s$) for caffeine as compared to phenol. For Phenomenex, the Henry constant of site 1 for caffeine is 2.44 ($2.44 = 0.95 \times 2.57$) and for phenol 1.30 ($a_1 = 1.371 \times 0.945 = 1.30$) [124]. However, the relatively larger contribution of caffeine to retention in site 1 interactions does not compensate for the effects of the relatively larger contribution to retention for phenol at the specific high-energy site, site 2. Also in the case of the low capacity interactions (site 2) the energy of interactions (b_2 terms) is about 2 times larger for caffeine as compared to phenol. However, the capacity terms at site 2 for caffeine are more than 10 times smaller as compared to phenol. For example, in the case of Phenomenex, $q_{s,2}$ is 0.059 mol/L for caffeine, as compared to the almost 15 times larger value of 0.87 mol/L for phenol. On the other hand, the energy of interaction at site 2 for phenol is almost 3 times smaller (b_2 is 9.11 L/mol for phenol as compared to 24.04 mol/L for caffeine). This means that the contribution to retention in the case of the Phenomenex column ($q_{s,2} \times b_2$) of site 2 for phenol is $a_2 = 7.92$, as compared to the retention contribution for caffeine, which is $a_2 = 1.42$; i.e. the retention contribution of phenol due to site 2 only, is more than 5 times larger than that of caffeine. This is illustrated by the more than 5 times larger grey rectangle for Phenomenex on the right-hand side of Fig. 13.

To conclude, the capacities of the low-energy sites for phenol are about twice those measured for caffeine, which is in agreement with the relative size of the two molecules. However, the saturation capacity of the high-energy sites is about 15 times larger for phenol as compared to caffeine and this suggests important differences in the structure of the two types of sites. These results allow an explanation for the paradoxical elution order of caffeine and phenol in the systems used [124]. The separation mechanism is based on the relative exclusion of the larger molecule of caffeine from the high-energy sites, rather than on the relative energy strength of the interactions. It is probable that the site 2 interactions are deeply buried in the C_{18}-bonded layer, indicating that in these cases the high-energy interactions do not derive their sources from silanols or dissociated silanophilic groups, exposed on the bare silica surface.

3.6.2.3. Characterization of hybrid phase systems. Many pharmaceuticals are heterocyclical amines and are classically associated with severe peak tailing at neutral or acidic pH. Neutral compounds are much easier to separate and are classically associated with high capacity and "Gaussian" analytical peaks. If the separation could be conducted at a pH well above the solute's pK_a, the amide would be uncharged and would act as a neutral compound. This is the background behind the great activity that has been aiming at pH-stable hybrid columns most recently.

In a recent investigation the aim was both to characterize such columns and to understand better the fundamental reasons for the large improvement in separation performance for basic solutes under alkaline conditions [125]. Four different C18 silica or hybrid silica/organic columns were investigated which, according to the manufacturer, were stable under alkaline conditions: Zorbax-Extend (pH 2–11.5), Gemini (pH 1–12), Hypersil GOLD (pH 2–10.6) and XBridge (pH 1–12). Three different probes were selected: a neutral 3-phenyl-1-propanol (PPR), an acidic 2-phenylbutyric acid (PB) and a basic metoprolol (ME). Firstly, a linear investigation was conducted with the pH between 3 and 11. The

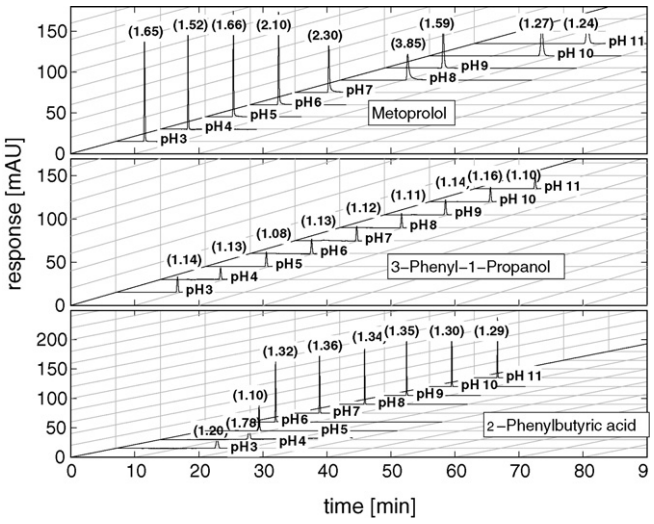

Fig. 14. The chromatograms for metoprolol (top), 3-phenyl-1-propanol (middle), and 2-phenylbutyric acid (bottom) for pH 3–11 on the XBridge column. The asymmetry values at 10% of peak height are inserted in parenthesis. Reprinted from Ref. [125], Copyright 2007, with permission from Elsevier.

investigation showed that, for all the columns, the retention time and asymmetry of the neutral probe PPR are unaffected by the pH, and that the symmetry for ME was much improved at pH > 9. The resulting peaks from the analytical investigation in the case of the XBridge column are shown in Fig. 14; the pH values are after each peak and the asymmetry factors (asf_{10}-values) are inserted in parentheses. The neutral PP showed constantly very symmetrical peaks throughout the entire pH-range. In the case of the acid PB, the asymmetry factor is approximately unity for all the pH values. This is because at higher pH values, the retention time is very short. For the base ME, the asymmetry factor is more or less below 2 at lower pH values and at its maximum at pH 8 ($asf_{10} = 3.85$); at higher pH > 9 very symmetrical and good peaks are obtained. The asymmetry of the ME peaks becomes close to unity at pH 10–11. The asymmetry was somewhat higher for the Extend column in the case of ME at high pH (not shown). The analytical investigation yields some insight into the adsorption isotherms. First it is seen that PP has no retention time changes due to pH or type of buffer system. This informs us that the distribution constants (the initial slope of the adsorption isotherm) are independent of the pH. As the asymmetry is near unity and no distinct change is present, one can conclude that the adsorption isotherm is more or less linear at low concentrations and does not change with the pH (due to conserved asymmetry values).

In the same study, a nonlinear investigation was also conducted at a pH of 3, 7 and 11 [125]. The data were collected and analyzed in the following way: (i) adsorption isotherm acquisition using FACP with the Cut-injection strategies [99]; (ii) raw data analysis with Scatchard plots and AED calculations; (iii) model fitting and comparison of models using the *F*-test, and finally (iv) analysis of overloaded injections. Like concluded from the analytical retention times, it was revealed that the adsorption isotherms of PP were unaffected by the pH. This is good, because for the interactions with the neutral probe we could conclude that the columns had not undergone any energetic change in the chromatographic process, at least from a neutral probes perspective. This is illustrated by the excellent reproducibility of the overloaded PP elution profiles using the XBridge column (see Fig. 15). This was not the case for PB and ME. Fig. 16 shows the elution profiles of overloaded injections of PB using the XBridge column; at pH 3 the peak is concentrated and has a good right-angled-triangular shape, like the PP peak (*cf.* Fig. 15). At pH 7 and 11 severe peak tailing appears and the separations at

3.6.2. ratio sepa- ctors.

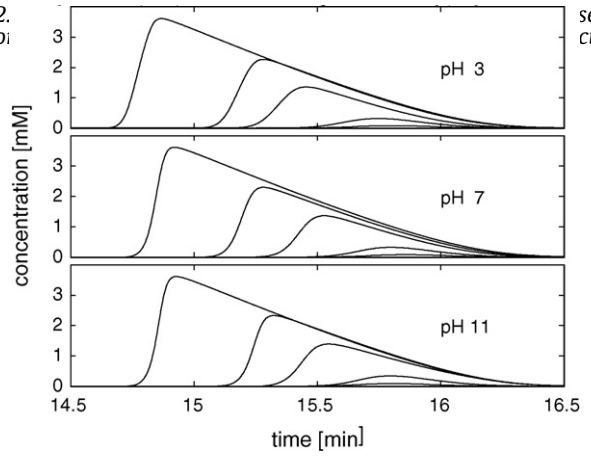

Fig. 15. 100 μL injection of 0.25, 1, 5, 10, and 20 mM 3-phenyl-1-propanol on the XBridge column. Top figure pH 3, middle pH 7, and bottom figure pH 11. Reprinted from Ref. [125], Copyright 2007, with permission from Elsevier.

this pH will increase the risk of compounds eluting with contaminants. The higher elution volumes also yield a diluted product, but the main issue is that the sample load is much lower compared to separations at pH 3, and this will decrease the productivity during the purification of PB in these conditions. The nonlinear adsorption investigation explained this feature; it was found that for all the columns the adsorption of PB was described with a Langmuir adsorption isotherm at pH 3 and with a bi-Langmuir adsorption isotherm at pH 7 and 11. At pH 7 and 11, the low capacity site (site 2) has approximately 2–5% of the total capacity and its equilibrium constant has around 70 times larger energy compared to the low-energy site (site 1). This is the explanation for more severe peak tailing in the case of charged acids [125].

In the case of the basic compound ME, bi-Langmuir isotherms described the adsorption at pH 3 and 11. However, at pH 11 the eluted peaks were much more compact right-angled-triangular peaks as compared with those at pH 3, see Fig. 17.

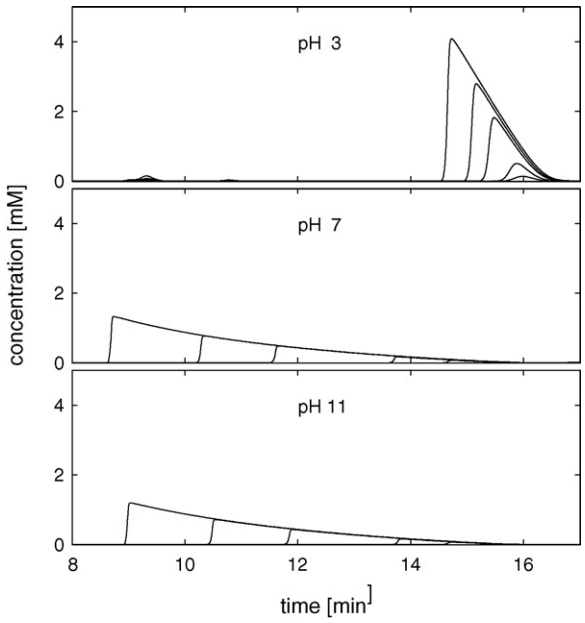

Fig. 16. 100 μL injection of 0.25, 1, 5, 10, and 20 mM 2-phenylbutyric acid on XBridge column. Top figure pH 3, middle pH 7, and bottom figure pH 11. Reprinted from Ref. [125], Copyright 2007, with permission from Elsevier.

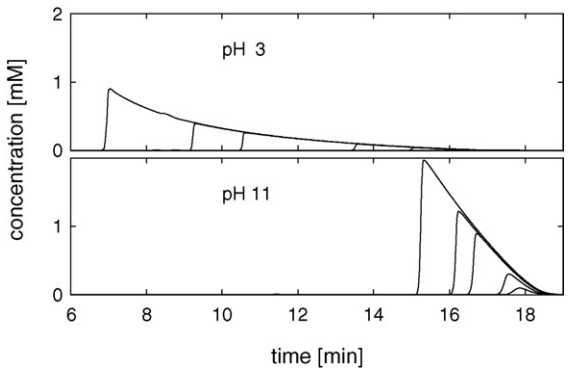

Fig. 17. 100 μL injection of 0.25, 1, 5, 10, and 20 mM metoprolol on the XBridge column. Top figure pH 3, and bottom figure pH 11. Reprinted from Ref. [125], Copyright 2007, with permission from Elsevier.

The explanation for why a bi-Langmuir adsorption at pH 11 gives a much better peak performance than a bi-Langmuir representation at pH 11 can be understood by interpenetration of the following histograms. In Fig. 18, histograms of the saturation capacities for bi-Langmuir fits of ME at pH 3 and pH 11 are presented. The total monolayer saturation capacity at pH 3 is approximately half of the monolayer saturation capacity at pH 11. The capacity for the high-energy site as compared to the total capacity is between 2% and 5% at pH 3 and around 20% at pH 11, for all the columns. The equilibrium constants of the strong site (site 2) are 55–100 times larger at pH 3 and only 6–7 times larger at pH 11, as compared to the low-energy equilibrium constant. Therefore, at pH 3, the eluted ME peaks will have similar properties to those of the eluted PB peaks at pH 7 and 11; severe peak tailing appears because of the low capacity of the high-energy site (site 2). On the other hand, at pH 11, the situation is different for ME; the adsorption energies are closer and the second site has a higher saturation capacity compared to pH 3. The second site at pH 11 will not be saturated as fast as the second site at pH 3. This will reduce the peak tailing and give rise to more compact peaks. This feature was very convincingly confirmed by the AED calculations of the adsorption of ME on the XBridge column at pH 11. The calculated adsorption energy distribution of the experimental raw adsorption isotherm is presented in Fig. 19; this AED is a classical bimodal distribution with 20% of the total capacity from the high-energy site. The equilibrium constant of the high-energy site is only 9 times larger than that of the low-energy site [125].

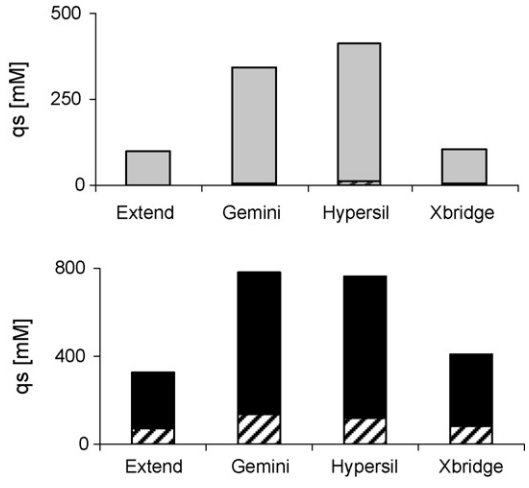

Fig. 18. Histograms showing the monolayer saturation capacities for metoprolol at pH 3 (top) and pH 11 (bottom) on all columns. The solid bar is for the low-energy site and the striped bar is for the high-energy site. Reprinted from Ref. [125], Copyright 2007, with permission from Elsevier.

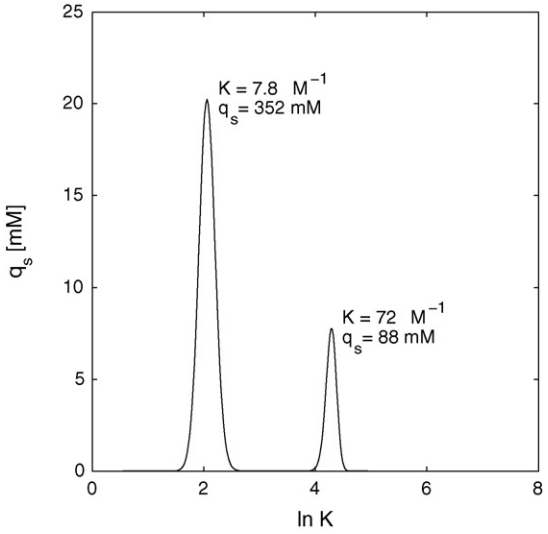

Fig. 19. Adsorption energy distribution from frontal analysis (step-series mode) from 25 μM to 100 mM in 30 steps for metoprolol tartrate using the XBridge column. Eluent: pH 11 with 0.3% ammonium hydroxide in 50% (v/v) methanol: buffer. 10^6 iterations were used. Reprinted from Ref. [125], Copyright 2007, with permission from Elsevier.

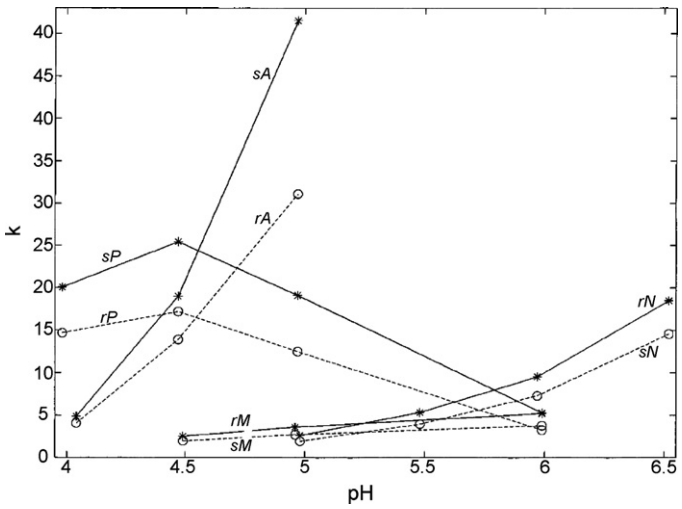

Fig. 20. Retention factors of the first (circles, dashed lines) and second eluted (asterisks, solid lines) enantiomer of the analytes versus the eluent pH. Experimental conditions: column, 100 × 4.0 mm; stationary phase, immobilized α_1-acid glycoprotein on silica; eluent, acetic buffer at I = 0.050 M and 0.25% 2-propanol; mobile phase flow rate, 0.80 mL/min; temperature, 20.0 °C; 20 μL of 0.050 mM racemates dissolved in eluent were injected. Analytes: (rA) (R)-alprenolol, (sA) (S)-alprenolol, (rP) (R)-2-phenylbutyric acid, (sP) (S)-2-phenylbutyric acid, (sM) (S)-methyl mandelate, (rM) (R)-methyl mandelate, (sN) (S)-1-(1-naphthyl)ethylamine, (rN) (R)-1-(1-naphthyl)ethylamine. Reproduced with permission from [127]. Copyright 2002 American Chemical Society.

The theory of nonlinear chromatography has successfully been used to characterize the chromatographic separation of the enantiomers of pharmaceutical drugs (often bases) on various types of immobilized proteins such as immobilized cellulose or α_1-acid glycoprotein, as stationary phases. In all the cases, it has been found that the thermodynamics of the adsorption of the drugs was heterogeneous; the enantiomers were adsorbed on one selective site of strong energy of interaction and on another, nonselective site of weak energy. In the case of the separation of the two enantiomers of the β-blocker propranolol on an immobilized cellulose protein, it was also found that the kinetics of the selective site was slower as compared to the kinetics of the nonselective site [126].

CHIRAL-AGP consists of α_1-acid glycoprotein immobilized on silica and is most popular due to its great stability and its great flexibility towards many different groups of chiral molecules and chiral drugs. One of the reasons for the flexibility is that the column can be operated for different solute groups at different pH values. Recently, a nonlinear investigation was made of the heterogeneous adsorption behaviour of selected chiral model compounds, at different mobile phase pH [127]. The solutes were two amines (alprenolol and 1-(1-naphthyl)ethylamine), one neutral (methyl mandelate) and one acid (2-phenylbutyric acid). Frontal analysis was used as method for determining the adsorption isotherms. Firstly, an analytical retention study was made versus the eluent pH for the various model compounds, and thereafter a deeper nonlinear investigation was made through adsorption isotherms in order to explain better the trends in the analytical investigation. The linear study showed that, when the eluent pH was increased, the "linear" retention factors of the amines increased strongly, especially for alprenolol (see Fig. 20), whereas the retention factors of the neutral increased very slightly. The retention factors of the acid showed a peculiar behaviour; the retention increased first and thereafter decreased with a maximum retention at pH 4.5. The nonlinear investigation showed that the surface was heterogeneous for all the compounds, having a small number of strong enantioselective adsorption sites and a larger number of weak nonselective ones [127]. The bi-Langmuir model fitted best to the data of all the compounds, giving individual estimates of the association equilibrium constants and the saturation capacities for both the non-chiral (K_I and $q_{s,I}$, respectively) and the chiral sites (K_{II} and $q_{s,II}$, respectively) for both the enantiomers. Remember that K and b are expressions for the same parameter, the association equilibrium constant (*cf.* Eqs. (6)–(9)). The saturation capacities can be seen in Table 2. Moreover, the adsorption studies showed that the trend for the amines was due to a strong increase in the enantioselective binding strength (K_{II}), whereas the retention of the neutral increased slightly as a result of an increase in both the enantioselective binding strength and its capacity (K_{II} and $q_{s,II}$). Interestingly, the nonlinear investigation revealed that the maximum retention of the acid shown in the linear study (*cf.* Fig. 7) originated solely from the enantioselective binding energy (K_{II}), whereas the strength of the nonselective energy (K_I) instead decreased steadily with increasing eluent pH (which is logical). For all the compounds, the enantioselective equilibrium constants increase relatively more than the nonselective ones with increasing pH. With increasing eluent pH, the interaction of both the enantiomers of both the amines at both types of sites was increased; however, the increase in the energy in the enantioselective interaction was much greater than that in the nonselective one. The values of the saturation capacities (*cf.* Table 2) allowed – when compared with the amount which the stationary phase determined – the calculation of the drug–protein stoichiometry. It was found that there was a 1:1 stoichiometry at the enantioselective site, while

Table 2
Non-chiral and chiral saturation capacities for the chiral stationary phase CHIRAL-AGP. $q_{s,1}$ and $q_{s,2}$ is the monolayer saturation capacity for the high capacity site (the non-selective site) and low capacity site (the enantioselective site), respectively. The mobile phase comprised of acetate buffer of pH 5.0, with ionic strength of 0.050 M. The table is adapted from Ref. [127].

Solute	Enantiomer	$q_{s,1}$ (mM)	$q_{s,2}$ (mM)	$q_{s,1}/q_{s,2}$
Alprenolol	R	9.7	3.02	3.2
Alprenolol	S	9.7	3.27	3.0
Methyl mandelate	R	12.6	2.15	5.9
Methyl mandelate	S	12.6	2.13	5.9
2-Phenylbutyric acid	R	29.4	3.60	8.2
2-Phenylbutyric acid	S	29.4	4.00	7.4

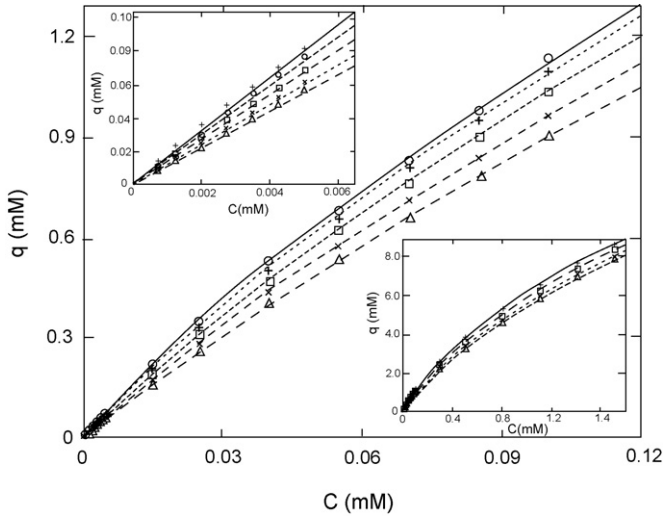

Fig. 21. Single-component equilibrium isotherms for (R)-propranolol at increasing temperatures. Symbols, experimental data; lines, calculated data using the best bi-Langmuir isotherms (Table 1). The figure shows the medium concentration range where the highest mobile phase concentration is 0.1 mM. The inset in the upper left corner shows the low-concentration range (below 5.0 μM), and the inset at the lower right corner the high-concentration range (up to 1.7 mM). Temperatures in K: (solid line) 278.15; (dotted line) 288.15; (dashed line) 298.15; (long dashed line) 308.15; (extra long dashed line) 318.15. Reproduced with permission from [74]. Copyright 1997 American Chemical Society.

the stoichiometry at the nonselective sites was more or less larger than 1 [127]. Moreover, the results demonstrated that ionic binding is very important for the enhancement of the chiral interaction using this protein CSP. On the other hand, the hydrophobicity of the molecule was found to play no significant role in the chiral interaction. Ionic interactions and hydrophobicity, on the other hand, play a role in the nonselective interactions of the basic drugs [128,129].

3.6.2.4.1. Derivation of thermodynamic quantities from nonlinear data. In the theoretical section in this review, it was explained that the thermodynamic functions ΔG°, ΔH°, and ΔS° of each site in a bi-Langmuir adsorption can be determined separately for the two types of sites. This procedure allows the direct determination of the chiral contributions to the isotherms and to the retention factors, of the thermodynamic functions of the chiral and non-chiral retention mechanisms, and of the true chiral separation factor.

This theory was applied to understand a most interesting temperature effect previously found to influence the analytical separation of the chiral β-blocker propranolol on an immobilized cellulase protein, cellobiohydrolase (Cel7A), as the stationary phase [74,129,130]. The unusual feature was that the retention factor of the more retained (S)-propranolol increases with increasing temperature, from 10 to 40 °C, while the retention of the less retained (R)-propranolol decreases [74]. To understand this behaviour, adsorption isotherms of R- and S-propranolol, respectively, were acquired in a wide concentration range and at different column temperatures. The overlaid adsorption isotherms acquired at different temperatures for S-propranolol showed a most interesting feature. At low concentrations corresponding to the initial slope of the isotherms, the order of the isotherms versus the temperature agreed with the analytical-size injections (inset at the upper left corner in Fig. 21); the adsorption isotherm acquired at the highest temperature is at the top and that acquired at the lowest temperature is at the bottom. This showed agreement with the unusual endothermic behaviour indicated from the analytical chromatograms. However, most interestingly, in the high concentration region of the adsorption isotherms, the opposite was true; the adsorption isotherm collected at the highest temperature was placed at the bottom and that collected at the lowest temperature at the top (inset at the lower right-hand corner in Fig. 21). This is the normal behaviour found in all concentration regions for the less retained R-propranolol. In an intermediate concentration range, the order of the adsorption isotherms for S-propranolol switches when going from low to high concentration regions, with a transition range at around 0.025 mM (main Fig. 21).

The underlying reason was revealed by the parameters of the best fit of the heterogeneous adsorption model (the bi-Langmuir equation) to the isotherms. The enantiomers of R- and S-propranolol were adsorbed (1) on one chiral site of strong energy of interaction (large K_{II}) and a low monolayer capacity (small $q_{s,II}$) and (2) on one non-chiral site of low energy of interaction (small K_I) but high capacity (large $q_{s,I}$). In the case of S-propranolol, the chiral active site showed an endothermic behaviour, whereas the non-chiral site was exothermic. The former interaction dominated at low concentrations, but was saturated at high concentrations, which is why the adsorption isotherms continuously switched from an endothermic to an exothermic order as the concentration was increased (*cf.* the transition range in Fig. 21 [74]). However, even in an analytical concentration range where the endothermic contribution dominated, exothermic non-chiral interactions also played a more or less important role; the reason is that, even if their interactions are weak, there are many such sites ($q_{s,I}$ is large). Therefore, if the thermodynamic characterization is based only on analytical peak retention data, the values of the thermodynamic quantities will be wrong and, furthermore, a complete picture of the different interactions and their individual thermodynamic behaviour will not be possible based on analytical data [74].

For didactic reasons, the thermodynamic quantities for this particular system were also derived from analytical retention data, in the classical way using Eq. (3) [74]. It was found that the van't Hoff plots of the analytical retention factor do not give thermodynamic functions which can be ascribed to any single retention mechanism, non-chiral or chiral. Thermodynamic data must be acquired in the nonlinear region of the isotherm. It is even incorrect to derive thermodynamic parameters directly from retention data acquired under analytical conditions in this system when we know that the retention factor results from a mixed mechanism.

3.6.2.5. Validation of an improved technique for nonlinear characterization: the Cut-injection technique. The elution by characteristic points (ECP) method is a fast and precise method for determination of the adsorption isotherms. As mentioned above, constraints must be made using the method: (i) the adsorption isotherm needs to be a type I or type III adsorption isotherm, (ii) the column efficiency needs to be high, because the model is derived from the ideal model and, finally, (iii) there is a need for close-to-rectangular injection-profiles. Surprisingly the ECP method has been used for years with traditional injection techniques producing large deviations from rectangular profiles. But, in a recent study a new injection procedure was introduced, in order to obtain an almost rectangular injection profile [131]; here also the large errors were investigated that takes place without using the proposed injection procedure. In a separation system, the total dead-volume will contribute to band broadening and result in a lowering of the efficiency. Not only does the column contain dead volumes, but so too do the connections between the injector and the detector. The dead-volumes between the column and the detector and between the injection-loop and the column are rather easily minimized. The loop itself is a mixing chamber, but acts somewhat differently as compared to other dead-volumes. During an injection, the first portion leaving the loop will have experienced less time in the system compared with the last portion. This will lead to a most heterogeneous injection profile distribution.

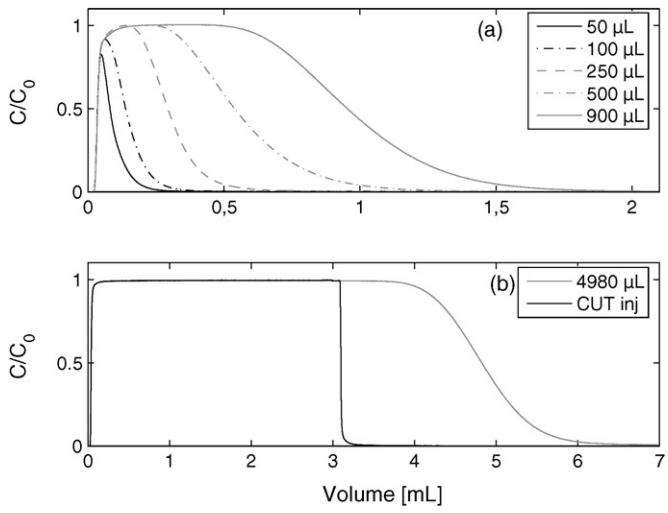

Fig. 22. Experimental injection-profiles for (a) different injection volumes between 50 and 900-μL aliquots and for (b) a 4980-μL traditional full-loop injection overlaid with the Cut-injection. For other experimental conditions, see Section 3.5.1. Reproduced with permission from [131]. Copyright 2008 American Chemical Society.

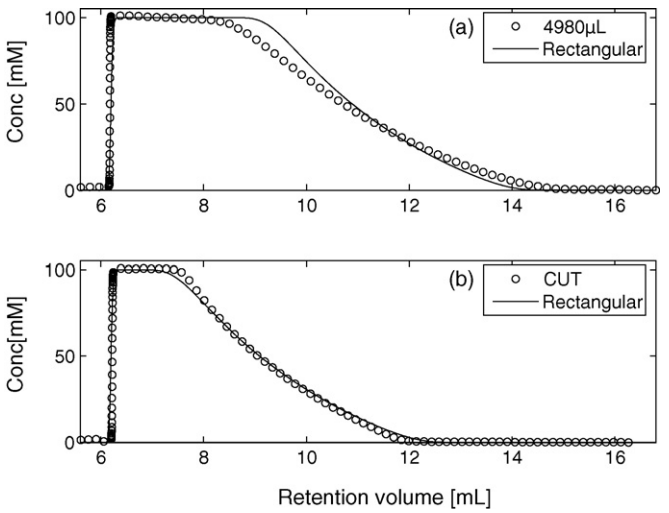

Fig. 24. Eluted chromatogram for a 100 mM injection of methyl mandelate resulting after (a) a 4980-μL full-loop injection and (b) a Cut-injection. The symbols are experimental data and the lines are simulations using a rectangular injection profile. Reproduced with permission from [131]. Copyright 2008 American Chemical Society.

In Fig. 22 experimental injection profiles are presented for different injection volumes. It is easy to see that the tail of the injection-profile becomes worse as the injection volume increases and that a stable concentration plateau is only established for very large injection volumes. The problem with large injection volumes is that the disperse tail of the injection-profile is larger. The front of the injection-profile is not as dispersed as the tail, since it has experienced lower mixing volumes. To improve the injection profile, the present authors [131] stopped the injection before the dispersed tail had entered the column by bypassing the loop; this is depicted in Fig. 23. In Fig. 19 the Cut-injection profile is presented in an overlaid fashion with the full-loop injection of 4980-μL. As can be seen from the figure, the injection-profile is much more like the rectangular injection-profile. To validate the effect of the injection-profile, an experimental chromatogram for 4980-μL full-loop injection and one for Cut-injection are compared with corresponding simulated elution profiles using rectangular injection-profiles, see Fig. 24 [131]. The results in Fig. 24 clearly show that using normal full-loop injection leads to a much more diffuse peak tail and that the result from the Cut-injection has a convincing overlap with elution profiles that are obtained with a rectangular injection-profile. This is a good indication that adsorption isotherms determined using the Cut-injection strategy should yield much more reliable adsorption data which was also proved recently [131]. In this context, its worthwhile mentioning that in recent theoretical and experimental applications of the inverse solver another approach is used to account for the injection profile [132–135]; however this is primar-

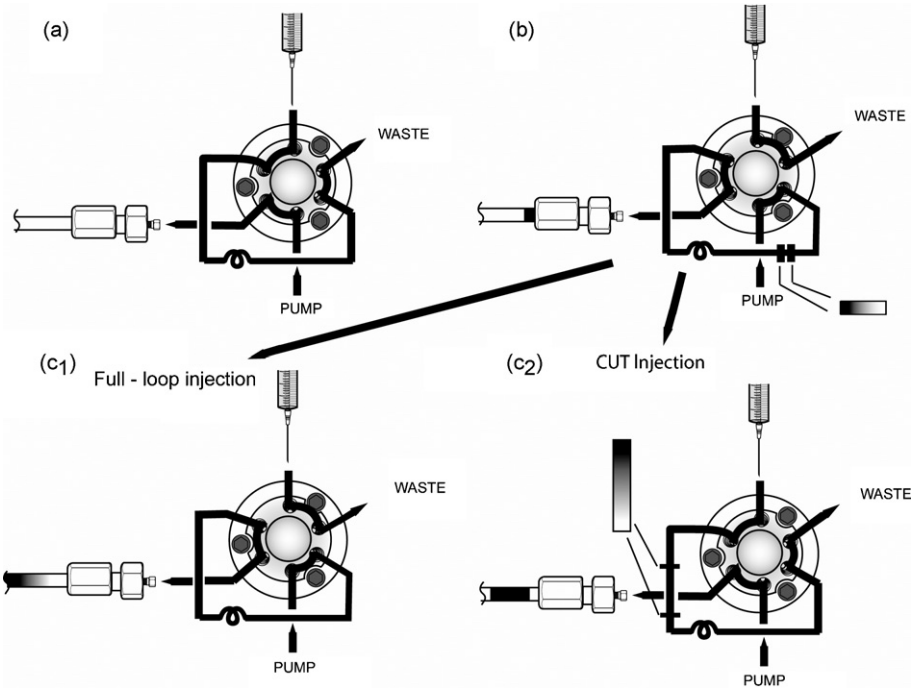

Fig. 23. A schematic representation of the events during the Cut-injection technique (*a*, *b* and c_2) compared with classical full-loop injection (*a*, *b* and c_1). Reproduced with permission from [131]. Copyright 2008 American Chemical Society.

ily for optimization of process chromatography, not in scope of this review.

4. Conclusions

The aim of this review is to give an overview and critical discussion of methods that provide a deeper understanding of the adsorption process and to exemplify, with the use of illustrative applications, what kind of knowledge can be achieved. The focus is placed on nonlinear methods, but two linear methods have also been selected, as they have a good potential for complementing the nonlinear methods, i.e. the linear solvation energy relationship (LSER) method and the hydrophobic-subtraction method (HSM). The adsorption isotherms contain the essential thermodynamic information about the interactions, but only if they are measured in a sufficiently broad concentration range and numerically treated and interpenetrated correctly. The reason for this is that different adsorption sites dominate differently at different concentration levels. Therefore, the application of too narrow a concentration range can falsely result in a homogeneous adsorption model. By numerical processing of the isotherms, the number of different interactions that take place simultaneously can be derived and the energy involved in each site can be determined. These results give a more complete understanding of the separation process than those of the traditional experiments assuming linear conditions and single site interactions.

The most updated methods for nonlinear characterization are described with their advantages and pitfalls, as well as references and illustrative examples of what kind of information can be gained on such a variety of system types, ranging from classical reversed-phase systems to hybrid systems and chiral separations. Through one of the new methods presented, the isotherm acquisition can be speeded up 10 times as compared to frontal analysis. This method is based on a technical improvement of a traditional method, the elution by characteristic point method (ECP). The adsorption isotherms acquired by using the new "Cut-technique" coincide perfectly with the adsorption isotherms determined by using the time-consuming frontal analysis method.

In order to select the "true" adsorption model, it is required that the raw isotherm data should be correctly treated and interpreted. A flow sheet is presented for a stringent model selection process. First a visual inspection is made of overloaded elution profiles. Thereafter Scatchard analysis is combined with calculations of the adsorption energy distribution (AED). AED calculations are a new and model-independent tool for revealing the actual number of adsorption interactions and their energy of interactions and monolayer capacities, without a priori assumption of any model. If this flow sheet is followed, it will narrow down considerably the number of possible models to fit to the data. Thereafter, the few possible models remaining are fitted to relevant rival models using nonlinear regression, and the best model is decided by means of a statistical *F*-test. Finally, the model and the determined adsorption isotherm parameter are validated by computer simulations in order to confirm that new experimental elution profiles can be properly predicted.

Finally, it is the hope of the author that this review can inspire the further development of methods for increased knowledge of the adsorption process. In this review convincing applications of the nonlinear methods have been demonstrated where the number of different interactions that take place simultaneously and the energy involved in each of these different types of interactions are determined. However, it is much more difficult, with only nonlinear methods, to identify which adsorption sites are electrostatic, acidic, basic, etc. Hopefully, the review should inspire advanced separation researchers to find a good way to achieve this, for example by combining nonlinear methods with linear ones such as LSERs and HSM.

Acknowledgments

The work was supported by a grant from the Swedish Research Council (VR) for the project "Fundamental Studies on Molecular Interactions Aimed at Preparative Separations and Biospecific Measurements".

References

[1] C.G. Horváth, B.A. Preiss, R.S. Lipsky, Anal. Chem. 39 (1967) 1422.
[2] G. Guiochon, J. Chromatogr. A 1168 (2007) 101.
[3] N. Vervoort, P. Gzil, G.V. Baron, G. Desmet, J. Chromatogr. A 1030 (2004) 177.
[4] H. Minakuchi, K. Nakanishi, N. Soga, N. Ishizuka, N. Tanaka, J. Chromatogr. A 762 (1997) 135.
[5] D.C. Hoth, J.G. Rivera, L.A. Colón, J. Chromatogr. A 1079 (2005) 392.
[6] S. Hjertén, J.L. Liao, R. Zhang, J. Chromatogr. 473 (1989) 273.
[7] K.K. Unger, N. Becker, P. Roumelites, J. Chromatogr. 125 (1976) 115.
[8] K.D. Wyndham, J.E. O'Gara, T.H. Walter, K.H. Glose, N.L. Lawrence, B.A. Alden, G.S. Izzo, C.J. Hudalla, P.C. Iraneta, Anal. Chem. 75 (2003) 6781.
[9] Gemini HPLC Mystery Solved Phenomenex 2005, booklet from Phenomenex.
[10] A.B. Scholten, J.W. de Haan, H.A. Claessens, L.J.M. van de Ven, C.A. Cramers, J. Chromatogr. A 688 (1994) 25.
[11] J.J. Kirkland, J.L. Glajch, R.D. Farell, Anal. Chem. 70 (1989) 4344.
[12] J.J. Kirkland, J. Chromatogr. A 1060 (2004) 9.
[13] J. Nawrocki, C. Dunlap, J. Li, C.V. McNeff, A. McCormick, P.W. Carr, J. Chromatogr. A 1028 (2004) 31.
[14] J. Nawrocki, C. Dunlap, A. McCormick, P.W. Carr, J. Chromatogr. A 1028 (2004) 1.
[15] J. Bowermasterm, H.M. McNair, J. Chromatogr. Sci. 22 (1984) 165.
[16] H.M. Chen, C. Horváth, J. Chromatogr. A 788 (1997) 51.
[17] Y. Yang, Anal. Chim. Acta 558 (2006) 7.
[18] P. Hemström, K. Irgum, J. Sep. Sci. 29 (2006) 1784.
[19] J.P. Alpert, J. Chromatogr. 499 (1990) 177.
[20] E.R. Francotte, J. Chromatogr. A 906 (2001) 379.
[21] J. Hermansson, M. Eriksson, J. Liq. Chromatogr. 9 (1986) 621.
[22] S. Allenmark, J. Liq. Chromatogr. 9 (1986) 425.
[23] I. Marle, A. Karlsson, C. Pettersson, J. Chromatogr. 604 (1992) 185.
[24] P. Erlandsson, I. Marle, L. Hansson, R. Isaksson, C. Pettersson, G. Pettersson, J. Am. Chem. Soc. 112 (1990) 4573.
[25] G. Götmar, J. Samuelsson, A. Karlsson, T. Fornstedt, J. Chromatogr. A 1156 (2007) 3.
[26] Y. Okamoto, Y. Kaida, J. Chromatogr. A 666 (1994) 403.
[27] Guidance for Industry PAT-A Framework for Innovative Pharmaceutical Development, Manufacturing, and Quality Assurance. U.S. Department of Health and Human Services, FDA, CDER, CVM, ORA, Pharmaceutical CGMPs September 2004.
[28] H. Colin, G. Guiochon, J. Chromatogr. 158 (1978) 183.
[29] F. Gritti, G. Guiochon, Anal. Chem. 77 (2005) 4257.
[30] R. Majors, Current Trends in HPLC Column Usage. http://chromatographyonline.findpharma.com/lcgc/ (2008 January 24).
[31] M. Kele, G. Guiochon, J. Chromatogr. A 830 (1999) 41.
[32] M. Kele, G. Guiochon, J. Chromatogr. A 830 (1999) 55.
[33] M. Kele, G. Guiochon, J. Chromatogr. A 855 (1999) 423.
[34] M. Kele, G. Guiochon, J. Chromatogr. A 869 (2000) 181.
[35] M. Kele, G. Guiochon, J. Chromatogr. A 913 (2001) 89.
[36] F. Gritti, G. Guiochon, J. Chromatogr. A 1003 (2003) 43.
[37] A. Felinger, G. Gritti, G. Guiochon, J. Chromatogr. A 1024 (2004) 21.
[38] L.R. Snyder, P.W. Carr, R.C. Rutan, J. Chromatogr. A 656 (1993) 537.
[39] H.A. Claessens, M.A. van Straten, M. Jezierska, B. Buszewski, J. Chromatogr. A 826 (1998) 135.
[40] D. Avnir, J. Am. Chem. Soc. 109 (1987) 2931.
[41] D. Farin, D. Avnir, J. Chromatogr. 406 (1987) 317.
[42] K.A. Lippa, L.C. Sander, J. Chromatogr. A 1128 (2006) 79.
[43] K.K. Unger, Packing and Stationary Phases in Chromatographic Techniques. Chromatographic Science Series, vol. 47, Marcel Dekker Inc., NY, USA, 1990.
[44] C. Stella, S. Heinisch, X. Liu c, P.-A. Carrupt, G. Cazorla, J.-Y. Gauvrit, P. Lantéri, K. Le Mapihan, J. Vial, S. Héron, A. Tchapla, J.-L. Rocca, J.-L. Veuthey, S. Rudaz, J. Pharm. Biomed. Anal. 39 (2005) 104.
[45] H. Engelhardt, M. Jungheim, Chromatographia 29 (1990) 59.
[46] K. Kimata, K. Iwaguchi, S. Onishi, K. Jinno, R. Eksteen, K. Hosoya, M. Araki, N. Tanaka, J. Chromatogr. Sci. 27 (1989) 721.
[47] M.J. Walter, J. Assoc. Off. Anal. Chem. 70 (1987) 465.
[48] S.V. Galushko, Chromatographia 46 (1993) 39.
[49] H.A. Claessens, M.A. van Straten, M. Jezierska, B. Buszewski, J. Chromatogr A 826 (1998) 135.
[50] M. Vitha, P.W. Carr, J. Chromatogr. A 1126 (2006) 143.
[51] L.R. Snyder, J.W. Dolan, P.W. Carr, J. Chromatogr. A 1060 (2004) 77.
[52] J.C. Giddings, H. Eyring, J. Phys. Chem. 59 (1955) 416.
[53] J.C. Giddings, Anal. Chem. 35 (1963) 1999.

[54] A. Felinger, A. Cavazzini, F. Dondi, J. Chromatogr. A 1043 (2004) 149.
[55] A. Felinger, J. Chromatogr. A 1184 (2008) 20.
[56] D.V. McCalley, Anal. Chem. 78 (2006) 2532.
[57] T. Greibrokk, T. Andersen, J. Chromatogr. A 1000 (2003) 743.
[58] G. Götmar, R.N. Albareda, T. Fornstedt, Anal. Chem. 74 (2002) 2950.
[59] G. Guiochon, A. Felinger, D.G. Shirazi, A.M. Katti, Fundamentals of Preparative and Nonlinear Chromatography, 2nd Ed., Academic Press imprint of Elsevier, Boston, MA, 2006.
[60] G. Guiochon, B. Lin, Modeling for Preparative Chromatography, 1st ed., Academic Press, San Diego, CA, 2003.
[61] C.F. Poole, S.K. Poole, J. Chromatogr. A 965 (2002) 263.
[62] N.S. Wilson, M.D. Nelson, J.W. Dolan, L.R. Snyder, R.G. Wolcott, P.W. Carr, J. Chromatogr. A 961 (2002) 171.
[63] T. Fornstedt, G. Zhong, G. Guiochon, J. Chromatogr. A 741 (1996) 1.
[64] T. Fornstedt, G. Zhong, G. Guiochon, J. Chromatogr. A 742 (1996) 55.
[65] A. Felinger, J. Chromatogr. A 1126 (2006) 120.
[66] I. Häglund, J. Ståhlberg, J. Chromatogr. A 761 (1997) 3.
[67] P. Szabelski, K. Kaczmarski, J. Chromatogr. A 1113 (2006) 74.
[68] K.S.W. Sing, D.H. Everett, R.A.W. Haul, L. Moscou, R.A. Pierotti, J. Rou-quérol, S. Siemieniewska, Pure Appl. Chem. 57 (1985) 603.
[69] G. Götmar, T. Fornstedt, G. Guiochon, Chirality 12 (2000) 558.
[70] F. Gritti, G. Guiochon, Anal. Chem 75 (2003) 5726.
[71] J. Lindholm, T. Fornstedt, J. Chromatogr. A 1095 (2005) 50.
[72] F. Gritti, G. Götmar, B.J. Stanley, G. Guiochon, J. Chromatogr. A 988 (2003) 185.
[73] M. Moreau, P. Valentin, C. Vidal-Madjar, B.C. Lin, G. Guiochon, J. Colloid Interface Sci. 141 (1991) 127.
[74] T. Fornstedt, P. Sajonz, G. Guiochon, J. Am. Chem. Soc. 119 (1997) 1254.
[75] A. Seidel-Morgenstern, J. Chromatogr. A 1037 (2004) 255.
[76] T. Herrmann, M. Schröder, J. Hubbuch, Biotechnol. Prog. 22 (2006) 914.
[77] P. Sajonz, G. Zhong, G. Guiochon, J. Chromatogr. A 731 (1996) 1.
[78] O. Lisec, P. Hugo, A. Seidel-Morgenstern, J. Chromatogr. A 908 (2001) 19.
[79] F. Helfferich, D.L. Peterson, Science 142 (1963) 661.
[80] F. Helfferich, J. Chem. Educ. 41 (1964) 410.
[81] J. Samuelsson, R. Arnell, J.S. Diesen, J. Tibbelin, A. Paptchikhine, T. Fornstedt, P.J.R. Sjöberg, Anal. Chem. 80 (2008) 2105.
[82] J. Samuelsson, R. Arnell, T. Fornstedt, Anal. Chem. 78 (2006) 2765.
[83] J. Samuelsson, P. Forssén, M. Stefansson, T. Fornstedt, Anal. Chem. 76 (2004) 953.
[84] A. Seidel-Morgenstern, G. Guiochon, J. Chromatogr. 631 (1993) 37.
[85] T. Fornstedt, G. Zhong, G. Guiochon, J. Chromatogr A 741 (1996) 1.
[86] P. Forssén, J. Lindholm, T. Fornstedt, J. Chromatogr. A 991 (2003) 21.
[87] H. Guan, B.J. Stanley, G. Guiochon, J. Chromatogr. A 659 (1994) 27.
[88] L. Ravald, T. Fornstedt, J. Chromatogr. A 908 (2001) 111.
[89] A. Felinger, A. Cavazzini, G. Guiochon, J. Chromatogr. A 986 (2003) 207.
[90] P. Forssén, R. Arnell, T. Fornstedt, Comput. Chem. Eng. 30 (2006) 1381.
[91] F. Gritti, G. Guiochon, J. Colloid Interface Sci. 264 (2003) 43.
[92] B.J. Stanley, J. Krance, J. Chromatogr. A 1011 (2003) 11.
[93] F. Gritti, G. Guiochon, J. Chromatogr. A 1043 (2004) 159.
[94] B.J. Stanley, S.E. Bialkowski, D.B. Marshall, Anal. Chem. 65 (1993) 259.
[95] B.J. Stanley, G. Guiochon, J. Phys. Chem. 97 (1993) 8098.
[96] J. Samuelsson, T. Fornstedt, J. Chromatogr. A 1203 (2008) 177.
[97] L.R. Snyder, J.W. Dolan, J.R. Gant, J. Chromatogr. 165 (1979) 3.
[98] F.D. Antia, C. Horváth, J. Chromatogr. 484 (1989) 1.
[99] G. Götmar, Heterogeneous Adsorption in Chiral LC. PhD thesis, Faculty of Pharmacy No 267, Uppsala University, Sweden, 2002.
[100] C.L. Baird, E.S. Courtenay, D.G. Myszka, Anal. Biochem. 310 (2002) 93.
[101] H. Xuan, D.S. Hage, Anal. Biochem. 346 (2005) 300.
[102] R.L. Rich, Y.S.N. Day, T.A. Morton, D.G. Myszka, Anal. Biochem. 296 (2001) 197.
[103] F. Gritti, G. Guiochon, J. Chromatogr. A 1097 (2005) 98.
[104] P. Sandblad, R. Arnell, J. Samuelsson, T. Fornstedt, Anal. Chem. 81 (2009) 3551.
[105] J. Samuelsson, P. Sajonz, T. Fornstedt, J. Chromatogr. A 1189 (2008) 19.
[106] J. Samuelsson, J. Zang, A. Murunga, T. Fornstedt, P. Sajonz, J. Chromatogr. A 1194 (2008) 205.
[107] K.J. Mayfield, R.A. Shalliker, H.J. Catchpoole, A.P. Sweeney, V. Wong, G. Guiochon, J. Chromatogr. A 1091 (2005) 124.
[108] S. Keunchkarian, M. Reta, L. Romero, C. Castells, J. Chromatogr. A 1119 (2006) 20;
K.J. Mayfield, R.A. Shalliker, H.J. Catchpoole, A.P. Sweeney, V. Wong, G. Guiochon, J. Chromatogr. A 1080 (2005) 124.
[109] H.J. Catchpoole, R.A. Shalliker, G.R. Dennis, G. Guiochon, J. Chromatogr. A 1117 (2006) 137.
[110] R.A. Shalliker, H.J. Catchpoole, G.R. Dennis, G. Guiochon, J. Chromatogr. A 1142 (2007) 48.
[111] R.A. Shalliker, G. Guiochon, J. Chromatogr. A 1216 (2009) 787.
[112] R.A. Shalliker, G. Guiochon, Bioprocess Int. 6 (9) (2008) 52.
[113] F. Khachkik, G.R. Beecher, J.T. Vanderslice, G. Furrow, Anal. Chem. 60 (1988) 807.
[114] P. Jandera, G. Guiochon, J. Chromatogr. 588 (1991) 1.
[115] J. Lindholm, P. Forssén, T. Fornstedt, Anal. Chem. 76 (2004) 4856.
[116] J. Lindholm, P. Forssén, T. Fornstedt, Anal. Chem. 76 (2004) 5472.
[117] L.R. Snyder, J.W. Dolan, P.W. Carr, J. Chromatogr A 1060 (2004) 77.
[118] J. Gilroy, J.W. Dolan, L.R. Snyder, J. Chromatogr. A 1000 (2003) 757.
[119] L.R. Snyder, A. Maule, A. Heebsch, R. Cuellar, S. Paulson, J. Carrano, L. Wrisley, C.C. Chan, N. Pearson, J.W. Dolan, J.J. Gilroy, J. Chromatogr. A 1057 (2004) 49.
[120] D.H. Marchand, L.R. Snyder, J.W. Dolan, Chromatogr. A 1191 (2008) 2.
[121] J.W. Dolan, L.R. Snyder, J. Chromatogr. A 1216 (2009) 3467.
[122] F. Gritti, G. Guiochon, J. Chromatogr. A 1038 (2004) 53.
[123] F. Gritti, G. Guiochon, Anal. Chem. 77 (2005) 1020.
[124] F. Gritti, G. Guiochon, Anal. Chem. 75 (2003) 5726.
[125] J. Samuelsson, A. Franz, B.J. Stanley, T. Fornstedt, J. Chromatogr. A 1163 (2007) 177.
[126] T. Fornstedt, G. Zhong, Z. Bensetiti, G. Guiochon, Anal. Chem. 68 (1996) 2370.
[127] G. Götmar, N.R. Albareda, T. Fornstedt, Anal. Chem. 74 (2002) 2950.
[128] G. Götmar, T. Fornstedt, M. Andersson, G. Guiochon, J. Chromatogr. A 905 (2001) 3.
[129] G. Götmar, T. Fornstedt, M. Andersson, G. Guiochon, J. Am. Chem. Soc. 121 (1999) 1164.
[130] T. Fornstedt, G. Guiochon, Anal. Chem. 73 (2001) 608A.
[131] J. Samuelsson, T. Fornstedt, Anal. Chem. 80 (2008) 7887.
[132] R. Arnell, P. Forssén, T. Fornstedt, Anal. Chem. 79 (2007) 5838.
[133] P. Forssén, R. Arnell, M. Kaspereit, A. Seidel-Morgenstern, T. Fornstedt, J. Chromatogr. A 1212 (2008) 89.
[134] R. Arnell, P. Forssén, T. Fornstedt, R. Sardella, M. Lämmerhofer, W. Linder, J. Chromatogr. A 1216 (2009) 3480.
[135] P. Forssén, R. Arnell, T. Fornstedt, J. Chromatogr. A 1216 (2009) 4719.